

Two-Phase Flow

12-1. INTRODUCTION

Two-phase flow phenomena are of utmost importance in liquid-cooled reactors. When a flowing coolant undergoes a partial change in phase, two-phase flow occurs, giving rise to interesting heat-transfer and fluid-flow problems. The phenomena occur regularly in boiling-water reactors, and in pressurized-water and other liquid-cooled reactors at high power densities. In general, two-phase flow implies the concurrent flow of two phases, such as liquid and its vapor (one component), liquid and gas (two component), gas and solid, etc. This chapter deals mainly with the first type, liquid and vapor flow. Flow in reactor channels, past restrictions, and critical flow will be discussed.

Two-phase flow takes several forms, shown in Fig. 12-1. These have been observed only in adiabatic two-phase, two-component flow, such as with air and water. However, there is good reason to believe that they exist in nonadiabatic two-phase flow. *Bubble flow* is the case in which individual dispersed bubbles move independently up the channel. *Plug*, or *slug*, *flow* is the case where patches of coalesced vapor fill most of the channel cross section as they move upward. *Plug flow* has been reported as being both a stable and an unstable transition flow between bubble flow and the next type, annular flow. In *annular flow* the vapor forms a

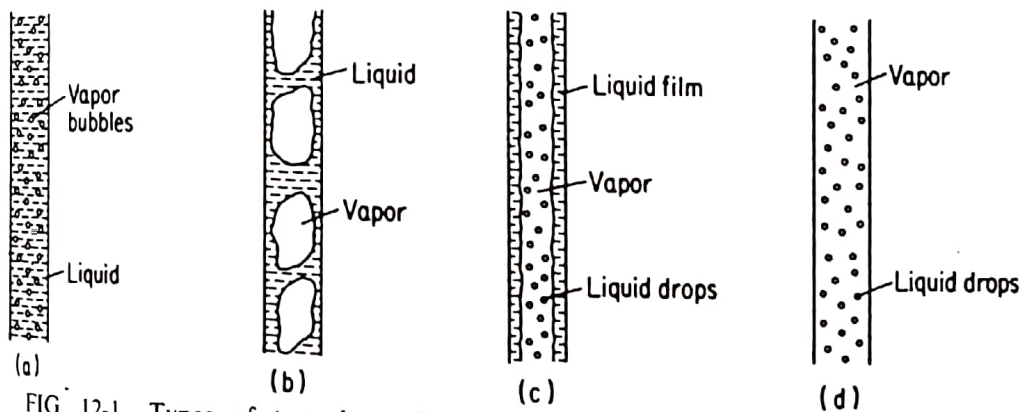


FIG. 12-1. Types of two-phase flow. (a) Bubble; (b) plug (slug); (c) annular (channelized); (d) fog.

continuous phase, carrying only dispersed liquid droplets, and travels up the channel core, leaving an annulus of superheated liquid adjacent to the walls. The fourth type shown in Fig. 12-1 is called *fog*, *dispersed*, or *homogeneous* flow. This is the opposite of the first type, bubble flow, in that in the latter case the vapor fills the entire channel and the liquid is dispersed throughout the vapor in the form of individual droplets.

Little is now known about the exact type of two-phase flow taking place in high-pressure reactor systems. It is conceivable, however, that it is determined by the *void fraction* (volumetric ratio of vapor to vapor and liquid). It is also believed that the type of flow is a function of the Froude number (a measure of the ratio of inertia to gravity forces).

12-2. QUALITY AND VOID FRACTION IN A NONFLOW SYSTEM

The importance of coolant-density and void-fraction studies in a boiling-reactor core will be discussed in Chapter 14. It suffices now to point out that, among several things, when a moderator boils, vapor voids displace this moderator and affect the reactivity of the system. Consequently only vapor of extremely low quality (a few percent) is to be produced in the core. The *quality* x of a vapor-liquid mixture in a nonflow system, or where no gross relative motion between the vapor and liquid phases exists, is defined as

$$x = \frac{\text{Mass of vapor in mixture}}{\text{Total mass of mixture}} \quad (12-1)$$

The *void fraction* α is defined as

$$\alpha = \frac{\text{Volume of vapor in mixture}}{\text{Total volume of liquid-vapor mixture}} \quad (12-2)$$

The term *void* here is somewhat misleading, since there is actually no void. However, the vapor present in "voids" has no moderating value because of its relatively low density.

The relationship between x and α in a nonflow system can be obtained by assuming a certain volume containing 1 lb_m of mixture in thermal equilibrium (Fig. 12-2). That volume will be equal to $(v_f + xv_{fg})$ ft³, where v is the specific volume (ft³/lb_m). In the notation used in this chapter, the subscripts f , g (below), and fg refer to saturated liquid, saturated vapor, and the difference between the two, respectively, the usual notation used in steam practice.

In an equilibrium mixture, the two phases are saturated liquid and saturated vapor and the volume of vapor present is equal to its mass, x lb_m, times its specific volume v_g . α is thus given by

$$\alpha = \frac{xv_g}{v_f + xv_g} \quad (12-3a)$$

This equation can also be written in the form

$$\alpha = \frac{1}{1 + \left(\frac{1-x}{x}\right) \left(\frac{v_f}{v_g}\right)} \quad (12-3b)$$

where the specific volumes are all taken at the system pressure from appropriate thermodynamic-property tables, such as the Keenan and Keyes steam tables in Appendix D. Equation 12-3b serves to show the large values of α associated with small values of x , especially at low pressures.

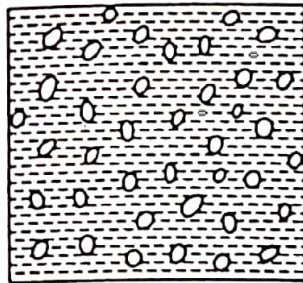


FIG. 12-2. A mixture of liquid and vapor in a nonflow system. Mass of mixture = 1 lb_m; composed of x lb_m saturated vapor plus $1 - x$ lb_m saturated liquid; volume of mixture = $v_f + xv_g$.

Example 12-1. Calculate α corresponding to $x = 2$ percent for ordinary water at atmospheric pressure.

Solution. From the steam tables, at atmospheric pressure,

$$v_f = 0.01672 \text{ ft}^3/\text{lb}_m \quad \text{and} \quad v_g = 26.800 \text{ ft}^3/\text{lb}_m$$

$$\alpha = \frac{1}{1 + [(1 - 0.02)/0.02]0.01672/26.800} = 0.971 \quad \text{or} \quad 97.1 \text{ percent}$$

Thus a small steam fraction by mass corresponds to a very large fraction by volume. The difference decreases at high pressure, however. Figure 12-3 shows calculated values for α versus x for light water at various pressures. Examination of the curves reveals the following:

1. For constant x , α decreases with pressure. As the pressure approaches the critical pressure (3,206 psia for ordinary water, 3,212 psia for heavy water) α rapidly approaches x . At the critical pressure the two phases are indistinguishable and $\alpha = x$.

2. For any one pressure, $d\alpha/dx$ decreases with x .

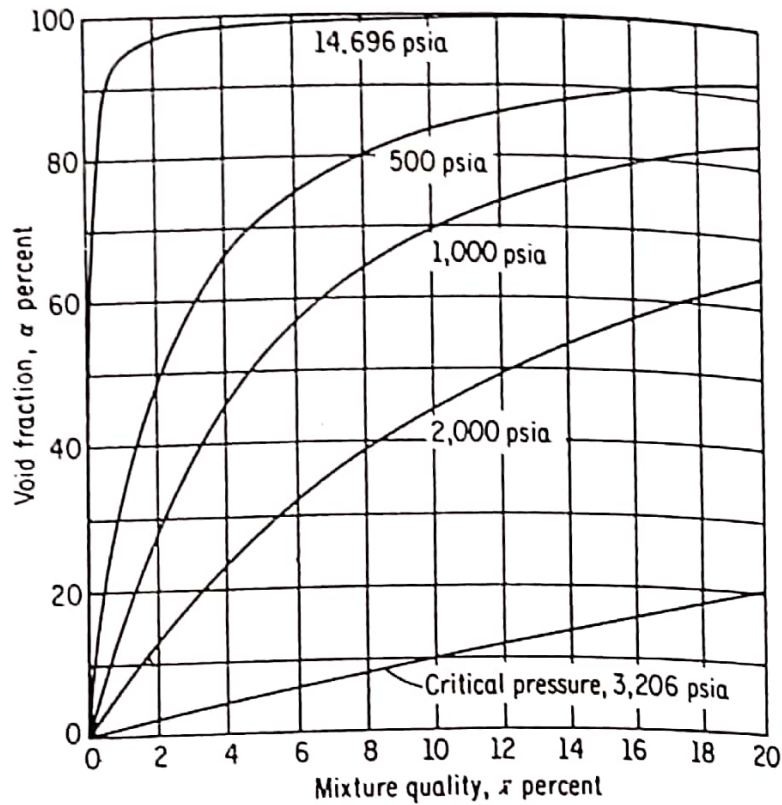


FIG. 12-3. α versus x for nonflow water system.

3. At low values of x (such as those used in boiling-type reactors), $d\alpha/dx$ increases as the pressure decreases and becomes very severely large at low pressure. This has a bearing on reactor stability [2].

12-3. THE FLOW SYSTEM

In the above calculations it was assumed that no relative motion existed between the two phases, i.e., between the vapor bubbles and the liquid. However, if a two-phase mixture is moving, say in a vertical direction as between fuel elements, the vapor, because of its buoyancy, has a tendency to slip past the liquid, i.e., move at a higher velocity than that of the liquid. While there are variations in velocity within each phase, no accurate method is now available to predict phase and velocity distributions in an actual two-phase flow system. The *lumped-system* solution in which each phase is assumed to move at one speed, however, has been found satisfactory in most cases. In the lumped system, a *slip ratio* S , equal to 1.0 in nonflow or homogeneous flow and greater than 1.0 in nonhomogeneous two-phase systems is used. It is defined as the ratio of the average velocity of the vapor V_g to that of the liquid V_f . Thus

$$S = \frac{V_g}{V_f} \quad (12-4)$$

The slip ratio modifies the relationship between void fraction and quality developed in the previous section. This will now be shown with the help of Fig. 12-4. Figure 12-4a shows a two-phase mixture flowing upward in a channel. A certain section, between the dotted lines, small enough so that x and α remain unchanged, is considered.

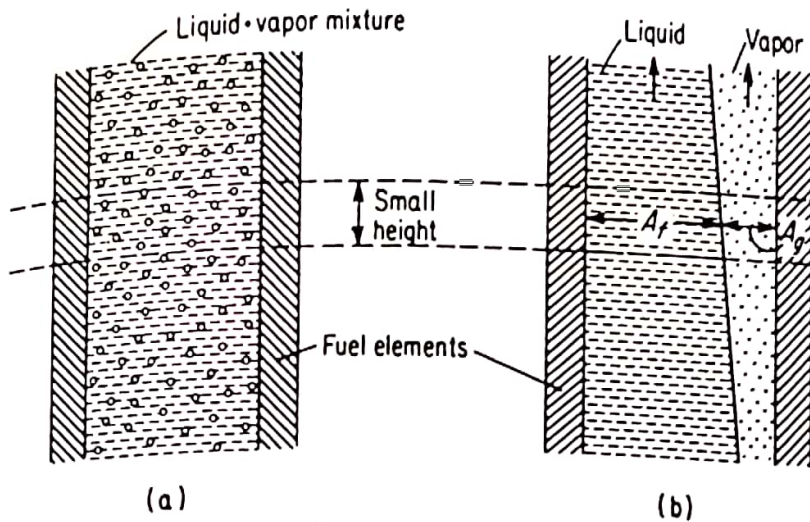


FIG. 12-4. Two-phase flow in a heated channel.

In a flow system, the quality at any one cross section is defined by

$$x = \frac{\text{Mass-flow rate of vapor}}{\text{Mass-flow rate of mixture}} \quad (12-5)$$

Thus if the total mass flow of the mixture is \dot{m}_t (lb_m/hr), the vapor-flow rate is $x\dot{m}_t$ and the liquid-flow rate is $(1-x)\dot{m}_t$, where x is the quality at the particular section in question. Applying the continuity equation, the velocities of vapor and liquid are given by

$$V_g = \frac{v_g \dot{m}_t}{A_g}$$

and

$$V_f = \frac{v_f (1-x) \dot{m}_t}{A_f}$$

where A_g and A_f are the cross-sectional areas of the two phases, perpendicular to flow direction, if the two phases are imagined to be completely separated from each other (Fig. 12-4b). Combining the above equations gives

$$S = \frac{V_g}{V_f} = \frac{x}{1-x} \frac{A_f}{A_g} \frac{v_g}{v_f} \quad (12-6)$$

The void fraction in the section considered is the ratio of the vapor-phase volume to the total volume within the section. In the small section of channel considered, this is the same as the ratio of cross-sectional area of vapor A_g to the total cross-sectional area of the channel. Thus

$$\alpha = \frac{A_g}{A_g + A_f}$$

or

$$\frac{A_f}{A_g} = \frac{1 - \alpha}{\alpha} \quad (12-7)$$

Equation 12-4a now becomes

$$S = \frac{x}{1 - x} \frac{1 - \alpha}{\alpha} \frac{v_g}{v_f} \quad (12-8)$$

This equation can be rearranged to give a relationship between α and x , including the effect of slip, as

$$\alpha = \frac{1}{1 + \left(\frac{1-x}{x}\right) \left(\frac{v_f}{v_g} S\right)} = \frac{1}{1 + \left(\frac{1-x}{x}\right) \psi} \quad (12-9)$$

and

$$x = \frac{1}{1 + \left(\frac{1-x}{x}\right) \frac{1}{\psi}} \quad (12-10)$$

where

$$\psi = \frac{v_f}{v_g} S \quad (12-11)$$

Note that the relationship between α and x for no slip ($S = 1$) given by Eqs. 12-3 is a special case of the general relationship given by Eqs. 12-9.

The effect of slip is to decrease the value of α corresponding to a certain value of x below that which exists for no slip. This can be seen if Eq. 12-9 is examined. At constant pressure and quality, the factor $(1 - \alpha)/\alpha$ is directly proportional to S . Thus, α decreases with S . A high S is thus an advantage from both the heat-transfer and moderating-effect standpoints. Figure 12-5 shows α versus x for light water at 1,000 psia and several slip ratios.

S has been experimentally found to decrease with both the system pressure and the volumetric flow rate and to increase with power density. It has also been found to increase with the quality at high

Two-Phase Flow

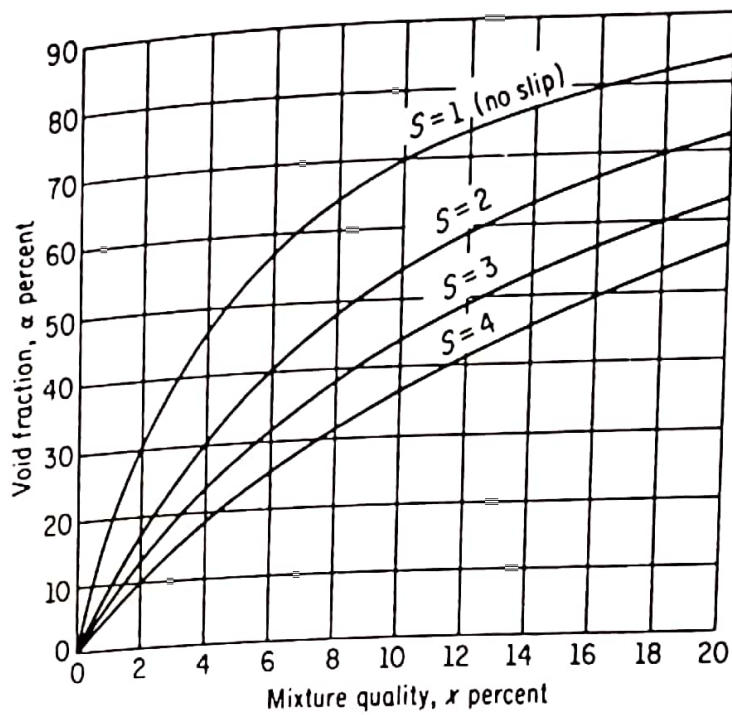


FIG. 12-5. α versus x for water at 1,000 psia and various slip ratios in a flow system.

pressures but to decrease with it at very low pressures [122]. Figures 12-6 to 12-8 show some of these effects. Figure 12-9 gives α versus $x\rho_f/\rho_g$ for various values of V_i^2/D , where V_i is the inlet velocity, at a pressure of 32 atm [123], from which S may be computed.

As a function of the channel length, S has been found to increase rapidly at the beginning and then more slowly as the channel exit is

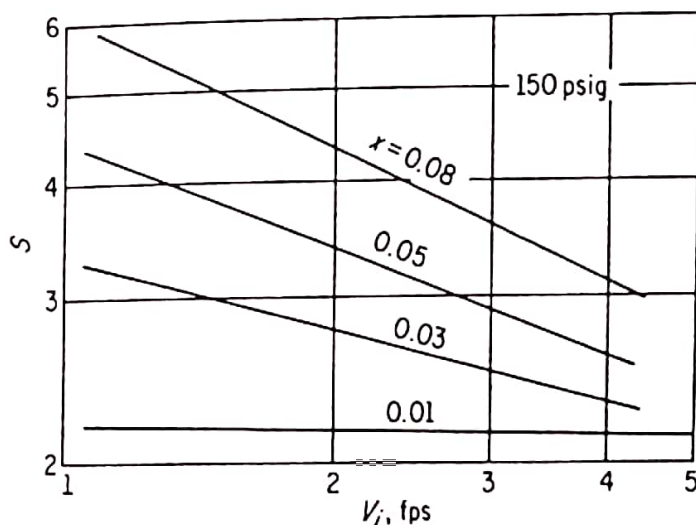


FIG. 12-6. Working curves for predicting slip ratios at 150 psig (Ref. 122).

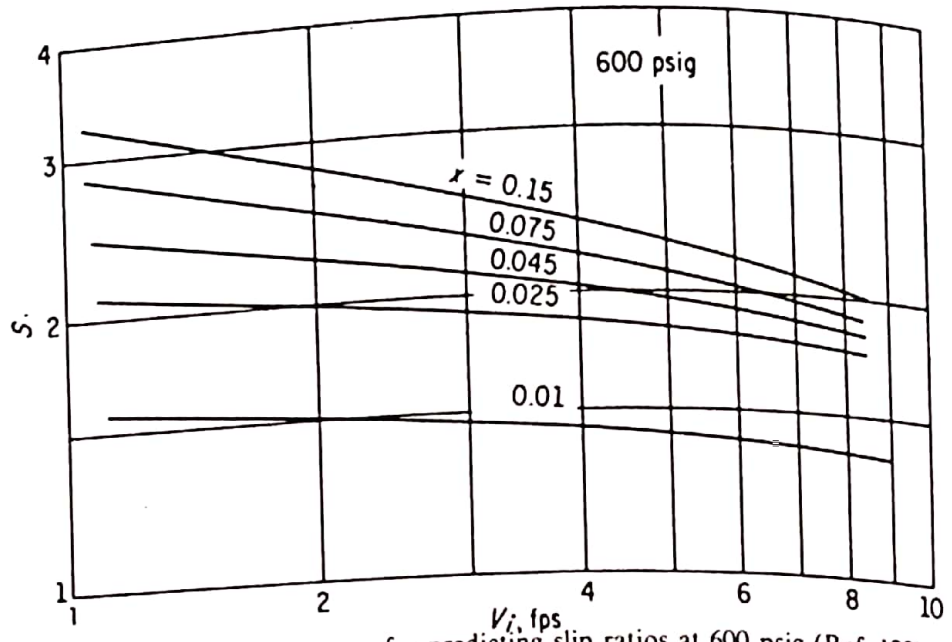


FIG. 12-7. Working curves for predicting slip ratios at 600 psig (Ref. 122):

approached. At the exit itself, turbulence seems to cause a sudden jump in the value of S . This effect is shown in Fig. 12-10 [124].

Von Glahn [125] proposed the following empirical relationship between x and α , based on much of the experimental data available at

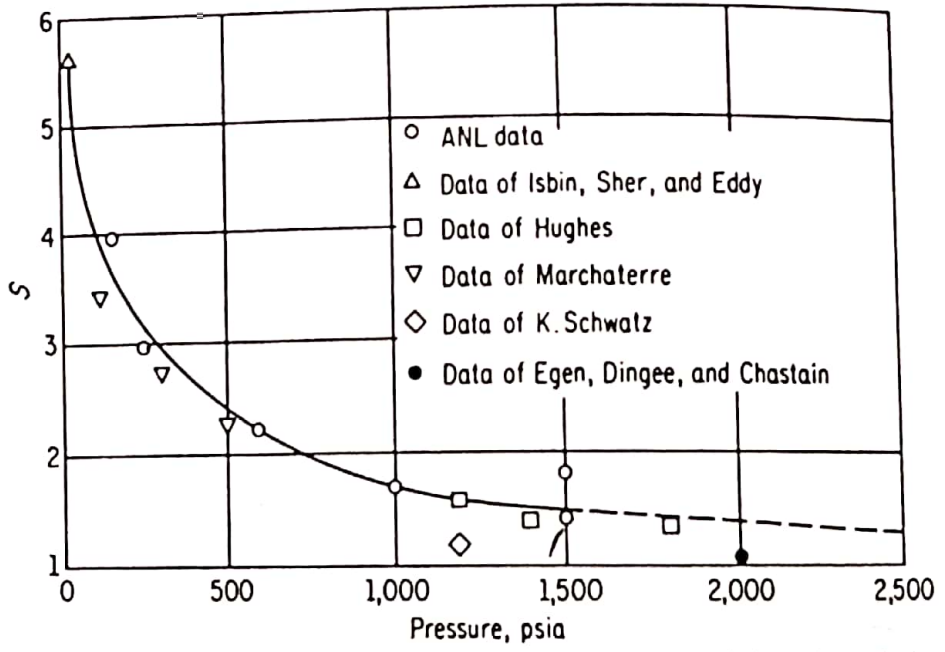


FIG. 12-8. Slip ratio as a function of pressure for $V_i \approx 2$ ft/sec and $x \approx 0.05$ (Ref. 122).

Two-Phase Flow

the time for water and covering a wide range of operating conditions and channel geometries:

$$\frac{1}{x} = 1 - \left(\frac{v_g}{v_f} \right)^{0.67} \left[1 - \left(\frac{1}{\alpha} \right)^{(v_g/v_f)^{0.1}} \right] \quad (12-12)$$

Experimental data or theoretical correlations for S covering all possible operating and design variables do not now exist. In boiling-reactor studies, values for S may be estimated from data that closely approach those of interest. In this a certain amount of individual judgment is necessary. Otherwise, experimental values of S under similar conditions of a particular design must be obtained. This procedure is usually expensive and time-consuming but may be necessary in some cases. The importance of obtaining accurate values of S may best be emphasized by the following: One step in the procedure of core channel design is to set a maximum value of α at the channel exit.

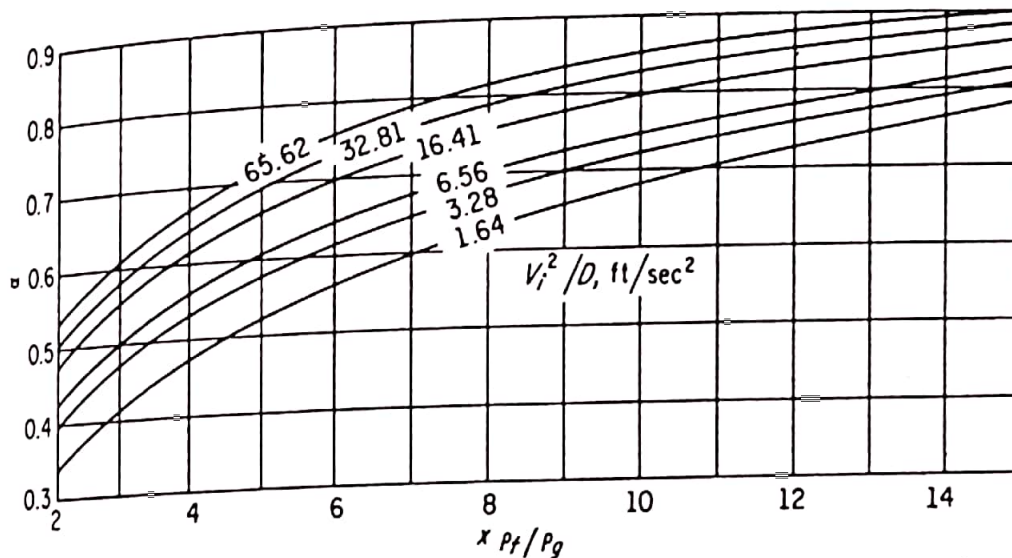


FIG. 12-9. Void fraction as a function of V_i^2/D and $x \rho_f / \rho_g$ for vertical tubes ($p = 32$ atm) (Ref. 123).

This is usually determined from nuclear (moderation) considerations. A corresponding value of x , at the selected S , is then found from the above equations. The latter determines the heat generated in the channel.

In design, the usual procedure is to assume a constant value of S along the length of the channel. This, of course, is a simplification, which may introduce further error into the results. In Fig. 12-10, however, S is seen to be fairly constant over most of the channel length, indicating this assumption to be a good one.

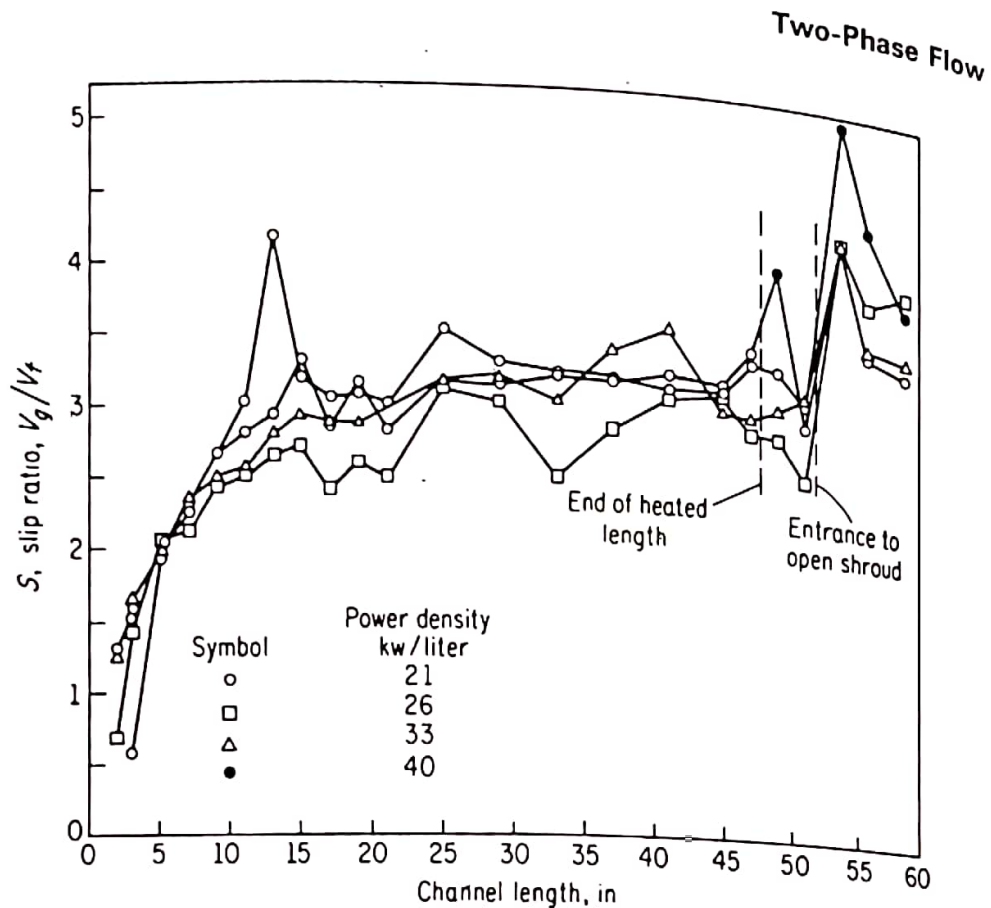


FIG. 12-10. Typical plots of slip ratio versus channel length at 114.9 psia (Ref. 124).

12-4. BOILING AND NONBOILING HEIGHTS

A boiling fluid in a flow system, such as a coolant flowing through the various channels of a boiling-reactor core, encounters several resistances to flow, manifesting themselves in pressure drops. Two of the largest are (1) the pressure drop due to friction (Sec. 12-5) and (2) the pressure drop caused by the acceleration of the coolant that undergoes an increase in volume as it receives heat in the channel (Sec. 12-6). Other pressure drops are due to the obstruction of flow by submerged bodies such as spacers, handles, tie plates, etc., and to abrupt changes in flow areas, such as at entrances and exits to the core, downcomers, etc. (Secs. 12-7 to 12-10).

In order to evaluate correctly the above-mentioned and other pressure drops as well as the average density in a boiling channel (necessary, among other things, for evaluating the driving head in a natural-circulation reactor), it is necessary to calculate the nonboiling height in the channel. The *nonboiling height* H_0 (Fig. 12-11) is that in which only the sensible heat is added to the incoming subcooled coolant at the channel bottom.

At $z = H_0$, the coolant becomes saturated. The remainder of the channel is that in which boiling takes place and is called the *boiling height* H_B .

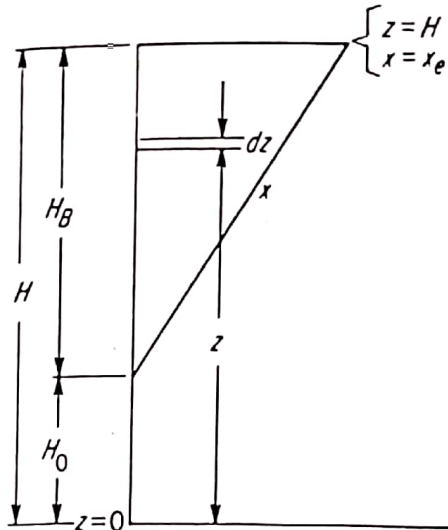


FIG. 12-11. Variation of quality with height in a uniformly heated channel.

Some subcooled boiling may, of course, occur in H_0 but will have little effect on pressure drops or density. The ratios H_0/H and H_B/H may be evaluated from the ratio of sensible heat added to total heat added in the channel:

$$\frac{q_s}{q_t} = \frac{h_f - h_i}{(h_f + x_e h_{fg}) - h_i} \quad (12-13)$$

where q_s = sensible heat added per pound mass of incoming coolant, Btu/lb_m

q_t = total heat added in channel per pound mass of incoming coolant, Btu/lb_m

h_i = enthalpy at inlet of channel, Btu/lb_m

The ratio q_s/q_t is related to the height ratio H_0/H according to the mode of heat addition in the channel. In the case of uniform heat addition (Fig. 12-11),

$$\frac{q_s}{q_t} = \frac{H_0}{H} \quad (12-14)$$

and $H_B/H = 1 - H_0/H$. In the case of sinusoidal heat addition, with extrapolation lengths neglected, Fig. 12-12, the area under the q''' or q' (heat added per unit length of channel) curve is proportional to q_t . The area

bounded by $z = 0$ and $z = H_0$ is equivalent to q_s . Thus

$$\frac{q_s}{q_t} = \frac{\int_0^{H_0} q'_c \sin(\pi z/H) dz}{\int_0^H q'_c \sin(\pi z/H) dz} = \frac{1}{2} \left(1 - \cos \frac{\pi H_0}{H} \right) \quad (12-15)$$

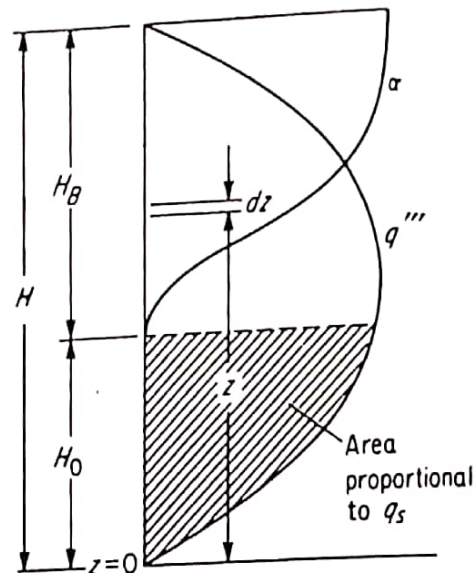


FIG. 12-12. Void fraction with sinusoidal heat addition in a boiling channel.

where q'_c is the heat addition per unit length of channel at the channel center, $z = H/2$, Btu/ft. H_0/H (and H_B/H) may then be evaluated from Eq. 12-15.

For other modes of heat addition that can be represented by a simple function, a similar procedure may be used. Otherwise, a stepwise or graphical solution becomes necessary.

12-5. THE FRICTION DROP IN A TWO-PHASE CHANNEL

The friction drop in a boiling channel of height H , $(\Delta p_f)_H$, is composed of friction due to single-phase (liquid) flow in H_0 , $(\Delta p_{sp})_{H_0}$, and two-phase flow in H_B , $(\Delta p_{TP})_{H_B}$, or

$$(\Delta p_f)_H = (\Delta p_{sp})_{H_0} + (\Delta p_{TP})_{H_B} \quad (12-16)$$

Single-Phase Friction

The single-phase friction pressure drop in H_0 , $(\Delta p_{sp})_{H_0}$, is evaluated by the standard methods used in single-phase flow, such as the Darcy formula. Thus

$$(\Delta p_{sp})_{H_0} = f_0 \frac{H_0}{D_e} \frac{\bar{\rho}_0 \bar{V}_0^2}{2g_c} \quad (12-17)$$

where f_0 = friction factor in H_0 , dependent upon average Reynolds' number and wall roughness in H_0 , dimensionless, (Appendix F)

D_e = equivalent diameter of channel, ft

$\bar{\rho}_0$ = average liquid density in H_0 , lb_m/ft^3

\bar{V}_0 = average liquid velocity in H_0 , ft/hr

g_c = conversion factor, $4.17 \times 10^8 \text{ lb}_m \text{ ft}/\text{lb}_f \text{ hr}^2$

$\bar{\rho}_0$ may be evaluated, for linear change in density in H_0 , or for small degrees of subcooling, quite closely from

$$\bar{\rho}_0 = \frac{1}{2} (\rho_i + \rho_f) = \frac{1}{2} \left(\frac{1}{v_i} + \frac{1}{v_f} \right) \quad (12-18)$$

where subscripts i and f again refer to channel inlet and liquid saturation. The specific volumes v_i and v_f are obtained at t_i and t_f respectively. Likewise \bar{V}_0 may be evaluated from

$$\bar{V}_0 = \frac{1}{2} (V_i + V_f) \quad (12-19a)$$

where V_f = the velocity of the saturated liquid at $z = H_0$. For a constant area channel and steady flow,

$$\bar{V}_0 = \frac{1}{2} V_i \left(1 + \frac{v_f}{v_i} \right) \quad (12-19b)$$

The average Reynolds number in H_0 , at which f_0 is evaluated is also given by

$$\overline{\text{Re}}_0 = \frac{D_e \bar{V}_0 \bar{\rho}_0}{\bar{\mu}_0} = \frac{D_e V_i \rho_i}{\bar{\mu}_0} \quad (12-20)$$

where $\bar{\mu}_0$, the average liquid viscosity, is obtained quite closely from $\frac{1}{2} (\mu_i + \mu_f)$.

Two-Phase Friction

Two-phase flow friction is greater than single-phase friction for the same height and mass-flow rate. The difference appears to be a function of the type of flow (see Fig. 12-1), and results from increased flow speeds. It is experimentally determined by measuring the total pressure drop in a two-phase flow system and subtracting calculated drops due to single phase in H_0 , acceleration (Sec. 12-6), and inlet, exit, contraction and expansion losses (Secs. 12-7 to 12-10).

The two-phase friction drop in H_B , $(\Delta p_{TP})_{H_B}$, is usually evaluated by first calculating a single-phase pressure drop in H_B assuming that only

saturated liquid of the same total mass-flow rate exists in the channel. This is given by

$$(\Delta p_{SP})_{H_B} = f_B \frac{H_B}{D_e} \frac{\rho_f V_{f_0}^2}{2g_c} \quad (12-21)$$

where f_B is the friction factor in H_B , a function of a single (liquid)-phase Reynolds number in H_B , $D_e \rho_f V_{f_0} / \mu_f = D_e \rho_i V_i / \mu_f$.

A *two-phase friction multiplier*, \bar{R} , greater than 1, is then multiplied by the above to give $(\Delta p_{TP})_{H_B}$. Thus

$$\bar{R} = \frac{(\Delta p_{TP})_{H_B}}{(\Delta p_{SP})_{H_B}} \quad (12-22)$$

and the total friction pressure drop in the channel, Eq. 12-16, is now given by

$$(\Delta p_f)_H = \left(f_0 \frac{H_0}{D_e} \frac{\bar{\rho}_0 \bar{V}_0^2}{2g_c} \right) + \bar{R} \left(f_B \frac{H_B}{D_e} \frac{\rho_f V_f^2}{2g_c} \right) \quad (12-23)$$

If the degree of subcooling is not too great, Eq. 12-23 could be written, with little error, in the form

$$(\Delta p_f)_H = \left(f_B \frac{\rho_f V_f^2}{2g_c D_e} \right) (H_0 + \bar{R} H_B) \quad (12-24)$$

Many attempts at finding a correlation for \bar{R} have been made with varying degrees of success. The most widely accepted correlation is that of Martinelli and Nelson [126]. It is based upon previous correlations of two-phase turbulent flow by Martinelli and represents an extrapolation of pressure-drop data obtained for isothermal flow of air and various liquids at low pressures and temperatures. The Martinelli-Nelson correlation is presented in the form of a chart (Fig. 12-13) giving \bar{R} as a function of pressure and exit quality.

As seen, the Martinelli-Nelson correlation shows that \bar{R} is a function of quality and pressure but is independent of mass flow rate. While that correlation is widely used at reactor operating conditions, an experimental investigation by Huang and El-Wakil [127] on a two-phase flow loop with electrically heated rods (simulating fuel elements) at low pressures and consequently high void fractions (as would be expected in a loss of pressure accident) has shown that the two-phase friction multiplier is a function of quality, pressure and also mass velocity at these conditions. It has also shown that the Martinelli-Nelson correlation greatly underestimates that multiplier under these same conditions. Figure 12-14 shows the two-phase friction multiplier at the relatively low pressures of 25, 35, and 50 psia for various mass flow rates, as well as the

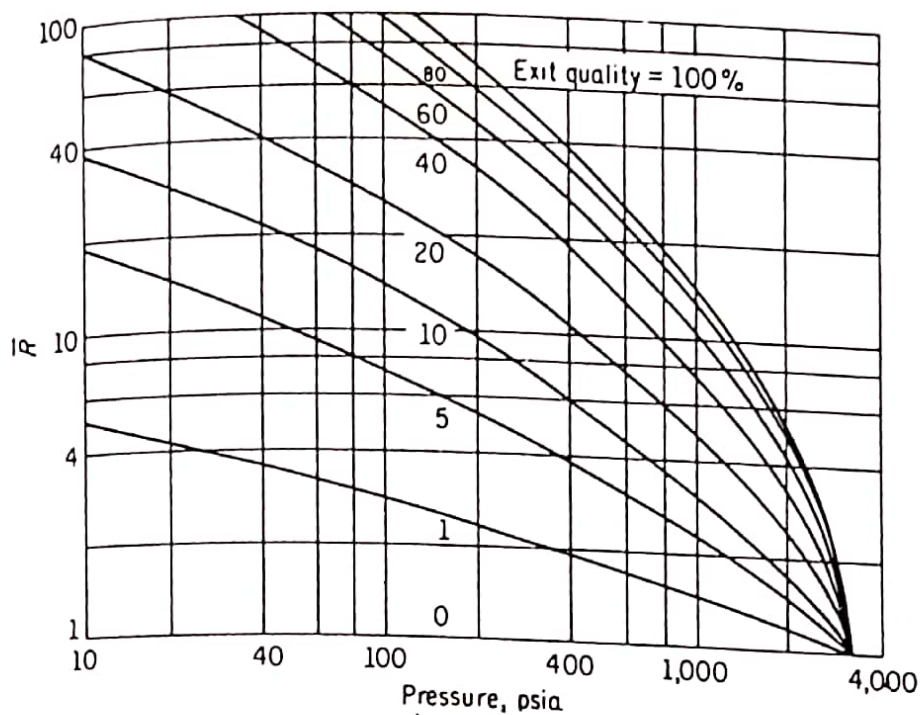


FIG. 12-13. Martinelli-Nelson friction-multiplier correlation (Ref. 126).

Martinelli-Nelson multiplier under the same conditions for comparison.

Another correlation for \bar{R} , given as a simple function of the exit void fraction, α_e , but one that lacks a pressure term in it, has been derived by Lottes and Flinn [128] on the basis of an annular-flow model (Fig. 12-1), uniform heating, and very low qualities. The model was conceived when plots of measured values of \bar{R} versus various parameters for a wide range of operating conditions but with uniform heat flux indicated that, for low qualities, \bar{R} is a function only of $1/(1 - \alpha_e)$.

It was theorized then that the increased friction drop was due to the increased liquid velocity caused by the reduced liquid flow area. Note that $1/(1 - \alpha_e)$ is the ratio of the total channel area to the liquid flow area at the exit. The friction in the annular-flow model considered would be mainly due to the friction between the liquid and the channel walls.

The above model is, of course, restrictive, and Lottes and Flinn reported later [129] that their correlation represents most data more qualitatively than quantitatively. Its derivation, however, is useful in understanding some two-phase flow concepts and will be presented here. Since the liquid velocity is variable along the channel, the Darcy formula is written in the differential form:

$$dp_{TP} = f_B \frac{\rho_f dz}{D_e} \frac{V_f^2(z)}{2g_c} \quad (12-25)$$

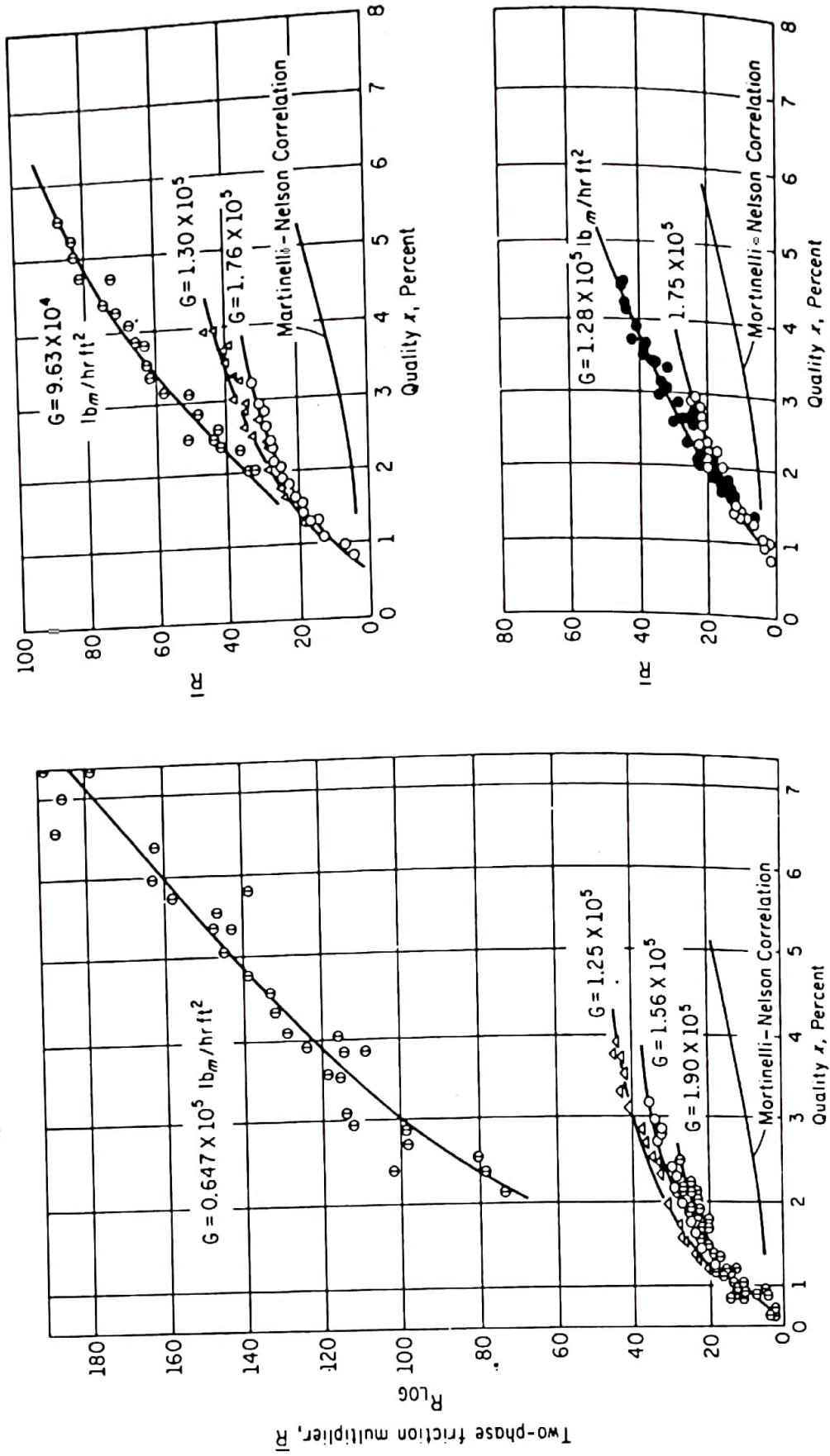


FIG. 12-14. El-Wakil-Huang two-phase friction multiplier at low pressures and high void fractions; left, 25 psia; top right, 35 psia; bottom right, 50 psia (Ref. 127).

Then

$$(\Delta p_{TP})_{H_B} = f_B \frac{\rho_f}{2g_c D_e} \int_{H_0}^H V_f^2(z) dz \quad (12-26a)$$

where $V_f(z)$ = speed of the saturated liquid at z , feet per hour and f_B = friction factor in H_B , assumed constant. To evaluate the integral, a relationship between $V_f(z)$, z and α_z , the void fraction at z , will be obtained. From the continuity equation, it can be shown that the mass-flow rates of the total mixture, \dot{m}_t , and of the saturated liquid at z , $\dot{m}_f(z)$, are given by

$$\dot{m}_t = V_{f_0} A \rho_f$$

and

$$\dot{m}_f(z) = (1 - x_z) \dot{m}_t = V_f(z) A (1 - \alpha_z) \rho_f$$

so that

$$\frac{V_f(z)}{V_{f_0}} = \frac{1 - x_z}{1 - \alpha_z} \quad (12-27)$$

where x_z is the quality at z .

For small values of x , $1 - x \cong 1$. Thus

$$(\Delta p_{TP})_{H_B} = f_B \frac{\rho_f V_{f_0}^2}{2g_c D_e} \int_{H_0}^H \frac{1}{(1 - \alpha_z)^2} dz \quad (12-26b)$$

For the case of uniform heat flux, the quality is a linear function of z , Fig. 12-11, or

$$x_z = x_e \frac{z - H_0}{H_B} \quad (12-28)$$

Equation 12-10 can be modified, for small values of x , to

$$x_z = \frac{\alpha_z}{1 - \alpha_z} \psi \quad (12-29)$$

and similarly

$$x_e = \frac{\alpha_e}{1 - \alpha_e} \psi \quad (12-30)$$

If S is assumed constant over H_B , Eqs. 12-28 to 12-30 can be combined to give

$$z - H_0 = \left(\frac{1 - \alpha_e}{\alpha_e} \right) \left(\frac{\alpha_z}{1 - \alpha_z} \right) H_B \quad (12-31)$$

from which

$$dz = \left(\frac{1 - \alpha_e}{\alpha_e} \right) \left(\frac{1}{1 - \alpha_z} \right)^2 H_B d\alpha_z \quad (12-32)$$

Substituting this equation in Eq. 12-26b gives

$$(\Delta p_{TP})_{H_B} = f_B \frac{H_B}{D_e} \frac{\rho_f V_{f_0}^2}{2g_c} \int_0^{\alpha_e} \left(\frac{1 - \alpha_e}{\alpha_e} \right) \left(\frac{1}{1 - \alpha_z} \right)^4 d\alpha_z \quad (12-26c)$$

The portion outside the integral sign on the right-hand side of the above equation is recognized as $(\Delta p_{SP})_{H_B}$, Eq. 12-21. The integral is therefore the two-phase multiplier \bar{R} . Thus

$$\begin{aligned} \bar{R} &= \left(\frac{1 - \alpha_e}{\alpha_e} \right) \int_0^{\alpha_e} \left(\frac{1}{1 - \alpha_z} \right)^4 d\alpha_z \\ &= \left(\frac{1 - \alpha_e}{\alpha_e} \right) \left[\frac{1}{3} \left(\frac{1}{1 - \alpha_z} \right)^3 \right]_{\alpha_z=0}^{\alpha_z=\alpha_e} \\ &= \left(\frac{1 - \alpha_e}{\alpha_e} \right) \left[\frac{1}{3} \left(\frac{1}{1 - \alpha_e} \right)^3 - \frac{1}{3} \right] \end{aligned} \quad (12-33a)$$

This equation can be rearranged to the more convenient form

$$\bar{R} = \frac{1}{3} \left[1 + \left(\frac{1}{1 - \alpha_e} \right) + \left(\frac{1}{1 - \alpha_e} \right)^2 \right] \quad (12-33b)$$

which is the Lottes-Flinn correlation for \bar{R} .

Example 12-2. A 6-ft-high boiling-water reactor channel has an equivalent diameter of 0.145 ft, and fuel cladding corresponding to smooth-drawn tubing. It receives heat sinusoidally and operates at a pressure of 1,000 psia, an exit quality of 8 percent, an inlet velocity of 3 fps, and inlet water temperature of 522°F. Compute the friction drop in the channel. Assume that the friction multipliers apply to sinusoidal heating.

Solution. Using Eq. 12-13 and the steam tables (Appendix D),

$$\frac{q_s}{q_t} = \frac{542.4 - 514.3}{(542.4 + 0.08 \times 649.4) - 514.3} = 0.351$$

Thus

$$0.351 = \frac{1}{2} \left(1 - \cos \frac{\pi H_0}{H} \right),$$

or

$$\cos \frac{\pi H_0}{H} = 0.298$$

from which $H_0/H = 0.404$, $H_0 = 2.424$ ft, and $H_B = 3.576$ ft.

We now evaluate f_0 at a Reynolds number corresponding to the average flow

conditions in H_0 . The product ρV is constant along the channel. The inlet liquid density ρ_i (at 522°F) is $1/v_i = 1/0.0209 = 47.847 \text{ lb}_m/\text{ft}^3$. Thus The inlet liquid

$$\text{Re}_0 = \frac{D_e \rho_i V_i}{\frac{1}{2} (\mu_f + \mu_i)} = \frac{0.145(3 \times 3600)47.847}{\frac{1}{2} (0.233 + 0.244)} = 314,165$$

where μ_f is evaluated by interpolation from Table E-1, Appendix. The relative roughness corresponding to smooth-drawn tubing is $0.000005/0.145 = 0.0000345$. Thus, from Appendix F,

$$f_0 = 0.0143$$

$$\rho_f = \frac{1}{v_f} = \frac{1}{0.0216} = 46.296 \text{ lb}_m/\text{ft}^3$$

$$\bar{\rho}_0 = \frac{1}{2} (\rho_i + \rho_f) = \frac{1}{2} (47.847 + 46.296) = 47.072 \text{ lb}_m/\text{ft}^3$$

$$V_{f_0} = V_i \frac{v_f}{v_i} = 3 \times \frac{0.0216}{0.02094} = 3.095$$

$$\bar{V}_0 = \frac{1}{2} (V_i + V_{f_0}) = \frac{1}{2} (3 + 3.095) = 3.047 \text{ fps}$$

The single-phase friction drop in H_0 is

$$\begin{aligned} (\Delta p_{SP})_{H_0} &= f_0 \frac{H_0}{D_e} \frac{\bar{\rho}_0 \bar{V}_0^2}{2g_c} = 0.0143 \frac{2.424}{0.145} \frac{47.072(3.047 \times 3600)^2}{2 \times 4.17 \times 10^8} \\ &= 1.623 \text{ lb}_f/\text{ft}^2 = 0.0113 \text{ lb}_f/\text{in}^2 \end{aligned}$$

To obtain the two-phase friction drop in H_B :

$$\text{Re}_B = \frac{D_e \rho_i V_i}{\mu_f} = \frac{0.145 \times 47.847(3 \times 3600)}{0.233} = 321,580$$

For the same roughness as above, and at Re_B , f_B is obtained from Appendix F.

$$f_B = 0.0142$$

The two-phase friction multiplier may now be obtained from the Martinelli-Nelson Chart, Fig. 12-13. Thus

$$\bar{R} = 2.8$$

The two-phase friction drop in H_B is

$$\begin{aligned} (\Delta p_{TB})_{H_B} &= \bar{R} f_B \frac{H_B}{D_e} \frac{\rho_f V_{f_0}^2}{2g_c} = 2.8 \times 0.0142 \frac{3.576}{0.145} \frac{46.296(3.095 \times 3600)^2}{2 \times 4.17 \times 10^8} \\ &= 1.756 \text{ lb}_f/\text{ft}^2 = 0.0469 \text{ lb}_f/\text{in}^2 \end{aligned}$$

Thus the total friction drop in the channel is

$$(\Delta p_f)_H = 0.0113 + 0.0469 = 0.0582 \text{ lb}_f/\text{in}^2$$

In the above case, the degree of subcooling is not too great and the above computations may be simplified by assuming all densities, viscosities and velocities to be those for saturated liquid. Thus

$$\begin{aligned}
 (\Delta p_f)_H &= f \frac{\rho_f V_{f_0}^2}{D_c 2g_c} (H_0 + \bar{R}H_B) \\
 &= 0.0143 \frac{46.296(3.095 \times 3600)^2}{0.145 \times 2 \times 4.17 \times 10^2} (2.424 + 2.8 \times 3.576) \\
 &= 8.452 \text{ lb}_f/\text{ft}^2 = 0.0587 \text{ lb}_f/\text{in}^2
 \end{aligned}
 \tag{12-24}$$

If the Lottes-Flinn correlation were to be used under these conditions, a value of slip ratio should first be obtained, as from Fig. 12-7. (A method of correcting S values for pressures other than the 600 psig shown is outlined by Marchaterre and Petrick [122].) Say $S = 1.9$.

Thus, for $x_e = 0.08$, α_e is obtained with the help of Eq. 12-9 as 0.486. Thus

$$\bar{R} = \frac{1}{3} \left[1 + \left(\frac{1}{1 - 0.486} \right) + \left(\frac{1}{1 - 0.486} \right)^2 \right] = 2.243$$

giving a total friction drop of 0.0493 psia.

12-6. THE ACCELERATION PRESSURE DROP

When a coolant expands (or contracts) because of heating, it has to accelerate as it travels through a channel. There will therefore be a force F equal to the change in momentum of the fluid. This force equals an *acceleration pressure drop* times the cross-sectional area of the channel. This pressure drop is usually small in single-phase flow, but can be quite large in two-phase flow. In reactor work where single-phase fluid enters the channel and two-phase fluid, with a high exit void fraction, leaves it, the change in momentum is particularly important. In such a case

$$F = \Delta p_a A_c = \frac{\dot{m}_f V_{fe}}{g_c} + \frac{\dot{m}_g V_{ge}}{g_c} - \frac{\dot{m}_i V_i}{g_c}
 \tag{12-34}$$

where Δp_a = acceleration pressure drop, due to change in momentum, between inlet and exit of channel, lb_f/ft^2

A_c = cross sectional area of channel, in square feet, assumed constant

$\dot{m}_i, \dot{m}_f, \dot{m}_g$ = total mass flow rate and mass-flow rates of saturated liquid and vapor, at exit of channel, lb_m/hr

V_i, V_{fe}, V_{ge} = velocities of water at inlet, of saturated liquid and of saturated vapor at exit, ft/hr

g_c = conversion factor, $4.17 \times 10^8 \text{ lb}_m \text{ft}/\text{lb}_f \text{hr}^2$

Equation 12-34 can be written in the form

$$\begin{aligned}\Delta p_a &= \frac{(1-x_e)\dot{m}_t V_{fe}}{g_c A_c} + \frac{x_e \dot{m}_t V_{ge}}{g_c A_c} - \frac{\dot{m}_t V_i}{g_c A_c} \\ &= \frac{G}{g_c} [(1-x_e)V_{fe} + x_e V_{ge} - V_i]\end{aligned}\quad (12-35)$$

where G = mass velocity = total mass-flow rate per unit cross-sectional area of channel = \dot{m}_t/A_c , ($\text{lb}_m/\text{hr ft}^2$), a constant quantity.

From the continuity equation,

$$V_{fe} = \frac{\dot{m}_f v_f}{A_{fe}} = \frac{(1-x_e)\dot{m}_t v_f}{A_{fe}} = \frac{(1-x_e)\dot{m}_t v_f}{(1-\alpha_e)A_c} = \frac{(1-x_e)G v_f}{1-\alpha_e}\quad (12-36)$$

Similarly,

$$V_{ge} = \frac{x_e G v_g}{\alpha_e}\quad (12-37)$$

and

$$V_i = G v_i\quad (12-38)$$

where A_{fe} = cross-sectional area of liquid at channel exit

v_f, v_g, v_i = specific volumes of saturated liquid, saturated vapor, and subcooled liquid at channel inlet.

Thus

$$\Delta p_a = \frac{G^2}{g_c} \left[\frac{(1-x_e)^2}{1-\alpha_e} v_f + \frac{x_e^2}{\alpha_e} v_g - v_i \right]\quad (12-39)$$

where x_e and α_e are related by Eqs. 12-9 and 12-10. Equation 12-39 is usually written in the form

$$\Delta p_a = r \frac{G^2}{g_c}\quad (12-40)$$

where r is an *acceleration multiplier*, having the units ft^3/lb_m and given by

$$r = \left[\frac{(1-x_e)^2}{1-\alpha_e} v_f + \frac{x_e^2}{\alpha_e} v_g - v_i \right]\quad (12-41)$$

The value of r increases rapidly with α and only slightly with S . It is independent of the mode of heat addition (uniform, sinusoidal, etc.) in the channel.

Example 12-3. Compute the acceleration pressure drop for the conditions of Example 12-2.

Solution

$$G = \rho_i V_i = 47.847(3 \times 3,600) = 0.5167 \times 10^6 \text{ lb}_m/\text{hr ft}^2$$

$$r = \left[\frac{(1-0.08)^2}{1-0.486} 0.0216 + \frac{0.08^2}{0.486} 0.4456 - 0.02094 \right] = 0.0205 \text{ ft}^3/\text{lb}_m$$

$$\Delta p_a = 0.0205 \frac{(0.5167 \times 10^6)^2}{4.17 \times 10^8} = 13.12 \text{ lb}_f/\text{ft}^2 = 0.0911 \text{ lb}_f/\text{in.}^2$$

12-7. TWO-PHASE FLOW PRESSURE DROP AT RESTRICTIONS

Two-phase mixtures commonly encounter sudden area changes, such as when they enter and leave fuel channels, pass by spacers, and others. These can be grouped under the headings abrupt expansion, abrupt contraction, orifices and nozzles. The pressure changes associated with these are usually small. Their magnitude could, however, as in natural-circulation systems, be large relative to the driving pressures (Sec. 14-4), and therefore must be evaluated as accurately as possible since they can materially influence coolant flow rates and consequently power output.

As with friction, these pressure changes are higher in two-phase than in single-phase flow because of the increased speed of the liquid caused by the presence of the voids. It also follows that the larger the void fraction, the larger the pressure change.

In the analysis it is necessary to evaluate integrated momentum and kinetic energy before and after the area change. These, however, cannot be evaluated with complete accuracy because detailed velocity distributions and the extent of equilibrium between the phases are not well known. Experimental data and empirical or semiempirical approaches are often resorted to.

The following analysis assumes (a) one-dimensional flow, (b) adiabatic flow across the area change, so that x is constant, and (c) pressure changes that are small compared to the total pressure so that ρ_f and ρ_g do not change (incompressible flow).

The following continuity equations, derived with reference to Fig. 12-4b, will aid in the analysis.

$$\begin{aligned} \text{In general,} \quad & \dot{m}_t = \rho A V \\ & \dot{m}_f = (1-x)\dot{m}_t = (1-\alpha)\rho_f A V_f \\ \text{and} \quad & \dot{m}_g = x\dot{m}_t = \alpha\rho_g A V_g \end{aligned} \quad \left. \vphantom{\begin{aligned} \dot{m}_t = \rho A V \\ \dot{m}_f = (1-x)\dot{m}_t = (1-\alpha)\rho_f A V_f \\ \dot{m}_g = x\dot{m}_t = \alpha\rho_g A V_g \end{aligned}} \right\} \quad (12-42)$$

$$\text{so that} \quad \left. \begin{aligned} V_{f_1} &= \frac{1-x}{1-\alpha_1} \frac{\dot{m}_t}{\rho_f A_1}, & V_{f_2} &= \frac{1-x}{1-\alpha_2} \frac{\dot{m}_t}{\rho_f A_2} \end{aligned} \right\} \quad (12-43)$$

$$\text{and} \quad \left. \begin{aligned} V_{g_1} &= \frac{x}{\alpha_1} \frac{\dot{m}_t}{\rho_g A_1}, & V_{g_2} &= \frac{x}{\alpha_2} \frac{\dot{m}_t}{\rho_g A_2} \end{aligned} \right\}$$

Two-Phase Flow

where the subscripts 1 and 2 refer to before and after the area change respectively.

It will be found instructive to begin the analysis with the case of single-phase incompressible flow, then follow up with the case of two-phase flow. This is the procedure that will be followed in each of the cases. The following three sections will deal with sudden expansions and contractions, and with orifices.

12-8. PRESSURE RISE DUE TO SUDDEN EXPANSION

Single-Phase Flow

For the case of *single-phase* flow, in a sudden expansion, Fig. 12-15,

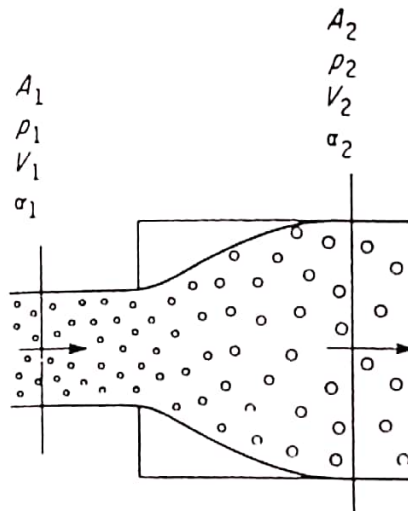


FIG. 12-15. Two-phase flow in sudden expansion.

the Bernoulli energy equation, written for incompressible ($\rho = \text{constant}$) one-dimensional* flow, is

$$p_1 + \frac{\rho V_1^2}{2g_c} = p_2 + \frac{\rho V_2^2}{2g_c} + k \frac{\rho V_1^2}{2g_c} \quad (12-44)$$

where the change in elevation between 1 and 2 is neglected and where all the terms have the dimensions of pressure. The last term represents a pressure loss because of viscous dissipation as the flow slows down. The symbol k is a dimensionless *loss coefficient*, also called the *Borda-Carnot coefficient*. Its value is obtained with the help of a momentum balance in which the upstream pressure p_1 is assumed to still act on the expanded

* This is an approximation, since the flow in this case is not truly one dimensional.

area A_2 immediately after expansion, since the flow lines there are essentially the same as at section 1. Thus

$$p_1 A_2 - p_2 A_2 = \frac{\dot{m}_t}{g_c} (V_2 - V_1) \quad (12-45a)$$

with the help of the continuity equation $\dot{m}_t = \rho A_2 V_2$, Eq. 12-45a may be written in the form

$$p_1 + \frac{\rho V_1 V_2}{g_c} = p_2 + \frac{\rho V_2^2}{g_c} \quad (12-45b)$$

Comparing Eqs. 12-44 and 12-45b gives

$$k \frac{\rho V_1^2}{2g_c} = \frac{\rho V_1^2}{2g_c} - \frac{\rho V_1 V_2}{g_c} + \frac{\rho V_2^2}{2g_c}$$

or

$$k = 1 - 2 \left(\frac{V_2}{V_1} \right) + \left(\frac{V_2}{V_1} \right)^2 = \left(1 - \frac{V_2}{V_1} \right)^2 = \left(1 - \frac{A_1}{A_2} \right)^2 \quad (12-46)$$

giving the pressure-loss term as

$$k \frac{\rho V_1^2}{2g_c} = \frac{\rho (V_1 - V_2)^2}{2g_c} \quad (12-47)$$

The total pressure change is obtained directly from Eq. 12-45b as

$$p_2 - p_1 = 2 \left[\frac{A_1}{A_2} - \left(\frac{A_1}{A_2} \right)^2 \right] \frac{\rho V_1^2}{2g_c} \quad (12-48a)$$

$$= \frac{1}{g_c} \left(\frac{1}{A_1 A_2} - \frac{1}{A_2^2} \right) \frac{\dot{m}_t^2}{\rho} \quad (12-48b)$$

or by combining Eqs. 12-44 and 12-46 to give

$$p_2 - p_1 = \frac{\rho (V_1^2 - V_2^2)}{2g_c} - \frac{\rho (V_1 - V_2)^2}{2g_c} \quad (12-48c)$$

Since A_1 is less than A_2 , the right-hand side of the above equation is positive, indicating a *net pressure rise* in the case of area expansion. This can be considered to be made of a pressure *rise* due to kinetic-energy change, obtained by putting $k = 0$ in Eq. 12-44 and given by the first term on the right-hand side of Eq. 12-48c, and a pressure *drop* due to viscous dissipation, given by the last term in Eq. 12-48c. This loss can be reduced in magnitude if the expansion were made gradual, to avoid flow separation, resulting in what is called a *subsonic diffuser*.

Two-Phase Flow

In two-phase flow, Fig. 12-15, several methods have been suggested for the calculation of the total pressure change across a sudden expansion. Lottes [130] compared four of these and recommended one by Romie. In this, a momentum balance is written assuming, as in single-phase above, that p_1 still acts on A_2 immediately after expansion, as follows

$$p_1 A_2 + \frac{\dot{m}_f V_{f_1}}{g_c} + \frac{\dot{m}_g V_{g_1}}{g_c} = p_2 A_2 + \frac{\dot{m}_f V_{f_2}}{g_c} + \frac{\dot{m}_g V_{g_2}}{g_c}$$

Using the relationships of 12-43 and rearranging give

$$p_2 - p_1 = \frac{\dot{m}_t^2}{g_c} \left\{ \frac{(1-x)^2}{\rho_f} \left[\frac{1}{(1-\alpha_1)A_1 A_2} - \frac{1}{(1-\alpha_2)A_2^2} \right] + \frac{x^2}{\rho_g} \left(\frac{1}{\alpha_1 A_1 A_2} - \frac{1}{\alpha_2 A_2^2} \right) \right\} \quad (12-49)$$

To evaluate the above equation, a relationship between α_2 and α_1 is needed. Based upon experiments by Petrick with air and water in vertical columns near atmospheric pressure, the following relationship was suggested:

$$\alpha_2 = \frac{1}{(p_2/p_1)[(1-\alpha_1)/\alpha_1](A_2/A_1)^{0.2} + 1} \quad (12-50)$$

α decreases somewhat across an expansion, with the percent decrease becoming smaller the higher the value of α_1 and the higher the area ratio. Table 12-2 shows values of α_2 vs. α_1 computed for $p_2/p_1 \approx 1$, the case of interest in reactor work. For area ratios 0.5 or larger, and high void fractions, the change may be ignored, i.e., $\alpha_1 = \alpha_2 = \alpha$, and Eq. 12-49 reduces to

$$p_2 - p_1 = \frac{1}{g_c} \left(\frac{1}{A_1 A_2} - \frac{1}{A_2^2} \right) \dot{m}_t^2 \left[\frac{(1-x)^2}{\rho_f(1-\alpha)} + \frac{x^2}{\rho_g \alpha} \right] \quad (12-51)$$

As in single-phase, there is a net pressure rise across an expansion. It can be seen that for the same mass-flow rate and areas, and since x is smaller than α , the pressure rise in two-phase flow, Eq. 12-51, is greater than in single-phase flow, Eqs. 12-48 and is larger the larger the void fraction. The two-phase equation 12-51 can be reduced to the single phase equation 12-48b by putting $x = 0$ and $\alpha = 0$.

TABLE 12-2
Effect of Area Expansion on Void Fraction
in Vertical Air-Water Mixtures*

A_1/A_2	α_1 , percent	α_2 , percent	Percent Change
0.2	10	7.4	-26
	20	15.3	-23.5
	40	32.0	-20
	60	52.0	-13.3
0.5	10	9.0	-10
	20	18.0	-10
	40	36.6	-8.5
	60	57.0	-5

* From Ref. 130.

12-9. PRESSURE DROP DUE TO SUDDEN CONTRACTION

In both single- and two-phase flow; area contractions result in *vena contracta* of area A_0 following the contraction (Fig. 12-16). The fluid then expands to the reduced area A_2 . The losses from the contraction to the vena contracta are negligibly small and the contraction losses are assumed to be totally due to the expansion from the vena contracta to where the fluid fills A_2 .

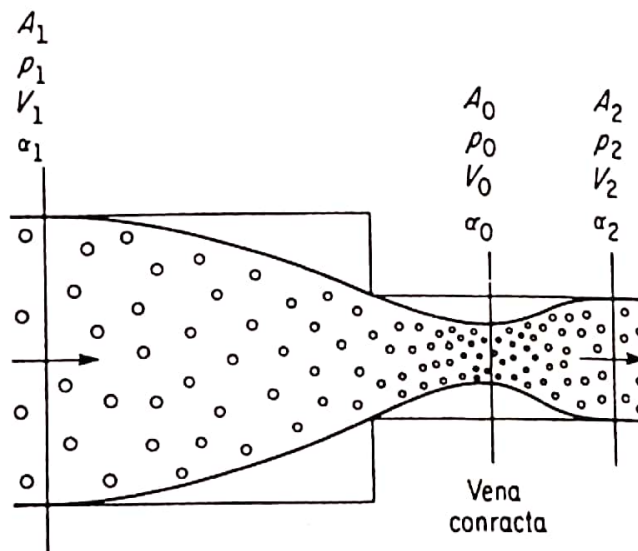


FIG. 12-16. Two-phase flow in sudden contraction.

Single-Phase Flow

Again, it is instructive to begin with *single-phase* flow. The pressure change in sudden contraction is given by a Bernoulli equation, similar to

Eq. 12-44 of sudden expansion, except that, since the losses are from the vena contracta to the reduce area, the loss term is customarily given in terms of the downstream velocity. Thus

$$p_1 + \frac{\rho V_1^2}{2g_c} = p_2 + \frac{\rho V_2^2}{2g_c} + k \frac{\rho V_2^2}{2g_c}$$

or

$$p_2 - p_1 = \frac{\rho(V_1^2 - V_2^2)}{2g_c} - k \frac{\rho V_2^2}{2g_c} \quad (12-52a)$$

$$= \left[1 - (k+1) \left(\frac{A_1}{A_2} \right)^2 \right] \frac{\rho V_1^2}{2g_c} \quad (12-52b)$$

k , the dimensionless loss-coefficient, is here a function of A_0 and A_2 and is given by

$$k = \left(\frac{A_2}{A_0} - 1 \right)^2 \quad (12-53)$$

Since A_0 is not known with certainty, k is usually given by

$$k = a \left[1 - \left(\frac{A_2}{A_1} \right)^2 \right] \quad (12-54)$$

where a is a dimensionless number, less than unity and reported variously between 0.4 and 0.5. Using 0.4 and combining Eqs. 12-52a and 12-54 and rearranging give

$$p_2 - p_1 = \frac{\rho(V_1^2 - V_2^2)}{2g_c} - 0.4 \left[1 - \left(\frac{A_2}{A_1} \right)^2 \right] \frac{\rho V_2^2}{2g_c} \quad (12-55a)$$

and since $A_1 V_1 = A_2 V_2$,

$$p_2 - p_1 = \frac{\rho(V_1^2 - V_2^2)}{2g_c} + 0.4 \frac{\rho(V_1^2 - V_2^2)}{2g_c} \quad (12-55b)$$

The above equation shows that the pressure change in sudden expansion is composed of a change of pressure due to change in kinetic energy and a loss term, which, in this case, is 40 percent of the kinetic energy term. Since $V_2 > V_1$ both terms are negative, so that sudden contractions result in a pressure drop. The above equations can be written in the convenient forms

$$p_2 - p_1 = 1.4 \left[1 - \left(\frac{A_1}{A_2} \right)^2 \right] \frac{\rho V_1^2}{2g_c} \quad (12-55c)$$

and

$$p_2 - p_1 = \frac{0.7}{g_c} \left(\frac{1}{A_1^2} - \frac{1}{A_2^2} \right) \frac{\dot{m}_1^2}{\rho} \quad (12-55d)$$

Two-Phase Flow

In *two-phase a* was found to be more nearly 0.2 [130]. Also the vapor is able to accelerate more readily than the liquid, resulting in a considerable decrease in the void fraction at the vena contracta. Beyond the vena contracta, however, shear forces between liquid and wall and between liquid and vapor steady the flow and cause α_2 to assume substantially the same value as α_1 so that $\alpha_1 = \alpha_2 = \alpha$. If ρ is replaced by the density of the two-phase mixture

$$\rho = (1 - \alpha)\rho_f + \alpha\rho_g \quad (12-56)$$

and the product $\alpha\rho_g$ is ignored, being relatively small at pressures far removed from critical, and if the pressure losses are attributed to the liquid alone, the pressure change in two-phase flow would be given by

$$p_2 - p_1 = 1.2 \left[1 - \left(\frac{A_1}{A_2} \right)^2 \right] \frac{\rho_f V_{f_1}^2}{2g_c} (1 - \alpha) \quad (12-57a)$$

or with the help of Eqs. 12-43, by

$$p_2 - p_1 = \frac{0.6}{g_c} \left(\frac{1}{A_1^2} - \frac{1}{A_2^2} \right) \frac{\dot{m}_t^2}{\rho_f} \frac{(1 - x)^2}{(1 - \alpha)} \quad (12-57b)$$

Since A_2 is less than A_1 , contractions result in pressure drops in both single- and two-phase flow. A comparison of Eqs. 12-55 and 12-57 shows that for the same mass-flow rate and areas, and for most values of x and α encountered in reactor work, the two-phase contraction pressure losses are larger than in single-phase and are larger the larger the void fraction.

12-10. TWO-PHASE FLOW IN ORIFICES

In general, the main object of orifices is to measure flow rates, which are functions of the square roots of pressure drops across them. Orifices, however, approximate many flow restrictions, such as spacers in reactor cores and others. It is the intent here to evaluate the pressure drop across orifices.

Single-Phase Flow

Starting as usual with *single phase*, the mass-flow rates for liquid and vapor are obtained from the continuity and energy equations, and given by the well-known equations

$$\dot{m}_f = A'_0 \sqrt{2g_c \rho_f (\Delta p_{SP})_f} \quad (12-58)$$

and

$$\dot{m}_g = A'_0 \sqrt{2g_c \rho_g (\Delta p_{SP})_g} \quad (12-59)$$

where

$$A'_0 = C_d \frac{A_0}{\sqrt{1 - \left(\frac{A_0}{A_c}\right)^2}} \quad (12-60)$$

(Δp_{SP}) is the single-phase pressure drop, A_0 and A_c are the cross sectional areas of the orifice and channel, Fig. 12-17, and C_d is a coefficient of discharge, obtained from experiments or published data [131] and is a function of the type of orifice, pressure-tap locations, etc.

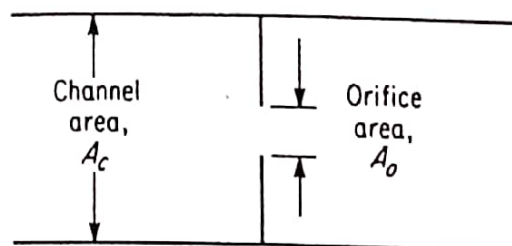


FIG. 12-17. Channel with thin plate orifice.

Two-Phase Flow

In *two-phase* flow, two similar expressions can be written for *coexistent* liquid and vapor phases of the above mass-flow rates as

$$\dot{m}_l = A'_{0l} \sqrt{2g_c \rho_l (\Delta p_{TP})_l} \quad (12-61)$$

and

$$\dot{m}_g = A'_{0g} \sqrt{2g_c \rho_g (\Delta p_{TP})_g} \quad (12-62)$$

$(\Delta p_{TP})_l$ and $(\Delta p_{TP})_g$ are the two-phase pressure drops due to liquid and vapor respectively. A'_{0l} and A'_{0g} are given by

$$A'_{0l} = C_d \frac{A_{0l}}{\sqrt{1 - \left(\frac{A_0}{A_c}\right)^2}} \quad (12-63)$$

and

$$A'_{0g} = C_d \frac{A_{0g}}{\sqrt{1 - \left(\frac{A_0}{A_c}\right)^2}} \quad (12-64)$$

where A_{0l} and A_{0g} are the flow areas within the orifice occupied by liquid and vapor respectively. Thus

$$A'_{of} + A'_{og} = C_d \frac{(A_{of} + A_{og})}{\sqrt{1 - \left(\frac{A_o}{A_c}\right)^2}}$$

and since $A_{of} + A_{og} = A_o$, comparison with Eq. 12-60 gives

$$A'_{of} + A'_{og} = A'_o \quad (12-65)$$

Assuming C_d does not change materially, Eqs. 12-58 to 12-62 can be combined with 12-65 to give

$$\sqrt{\frac{(\Delta p_{SP})_f}{(\Delta p_{TP})_f}} + \sqrt{\frac{(\Delta p_{SP})_g}{(\Delta p_{TP})_g}} = 1$$

Noting that $(\Delta p_{TP})_f$ and $(\Delta p_{TP})_g$ must both be equal to a two-phase pressure drop Δp_{TP} , the above equation reduces to

$$\sqrt{\Delta p_{TP}} = \sqrt{(\Delta p_{SP})_f} + \sqrt{(\Delta p_{SP})_g} \quad (12-66)$$

Δp_{TP} is therefore simply obtained from calculated pressure drops of the liquid and vapor phases as if they were flowing alone through the orifice. Their respective flow rates are obtained from the total flow rate and quality.

Experimental work by Murdock [132] on a wide range of operating conditions, showed that the above equation should be modified to

$$\sqrt{\Delta p_{TP}} = 1.26 \sqrt{(\Delta p_{SP})_f} + \sqrt{(\Delta p_{SP})_g} \quad (12-67)$$

12-11. CRITICAL FLOW

When the back pressure p_b is reduced below a constant upstream pressure p_o in a flow system, line 1 in Fig. 12-18, flow begins and a pressure gradient is established in the connecting channel between p_o and a pressure p_e at the exit of the channel. The flow increases as p_b is reduced further, line 2. p_e remains equal to p_b to a point. This point, represented by line 3, is reached when p_b is reduced sufficiently to cause the flow velocity at the exit of the channel to equal that of the speed of sound at the temperature and pressure at the exit of the channel, V^* . At that point the mass flow attains a maximum value.

Further reduction in p_b results in no further increase in mass flow rate or decrease in p_e , lines 4 and 5. The flow remains at the above maximum value and is said to be *critical*. The channel, and flow, are also said to be *restricted* or *choked*. As p_b is reduced and p_e remains constant, free expansion of the fluid between p_e and p_b occurs outside the channel and the flow takes on a paraboloid shape there.

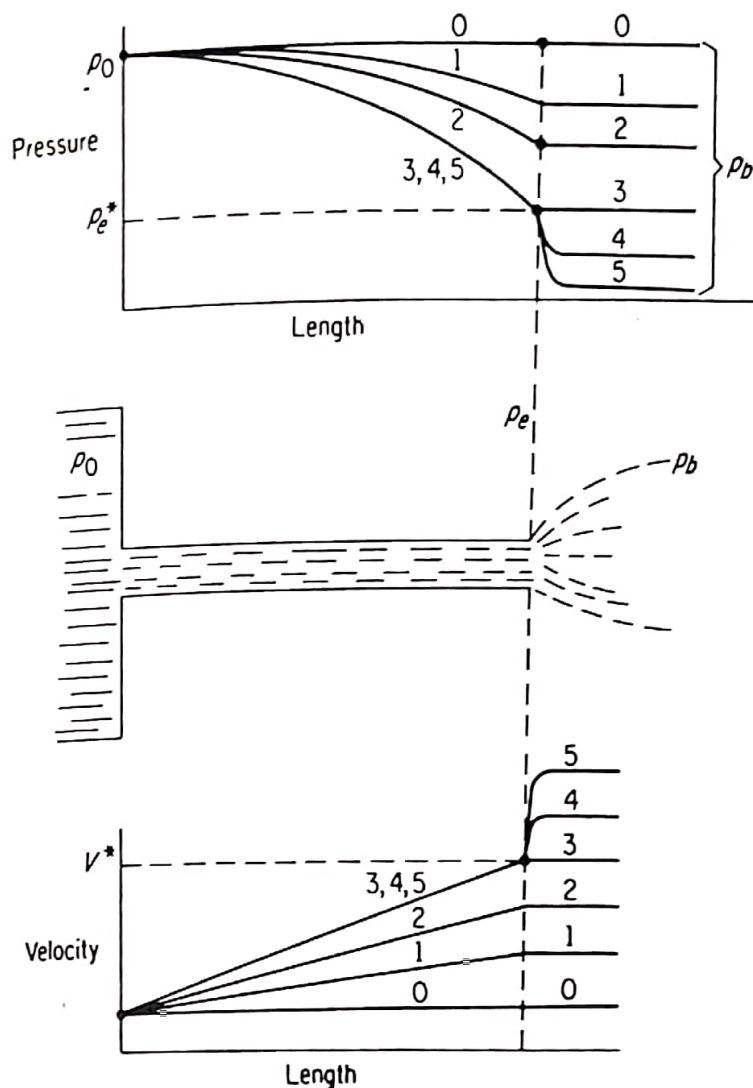


FIG. 12-18. Critical flow model.

This phenomenon occurs in both single- and two-phase flow. It has been well studied in single-phase, particularly gas flow, both theoretically and experimentally. It occurs, and is utilized, in many flow and measuring systems. In two-phase flow, serious theoretical and experimental studies of the phenomenon have been made only in recent years, although the phenomenon has long been observed in boiler and turbine systems, flow of refrigerants and rocket propellants, and many others.

In nuclear work, the phenomenon is of utmost importance in safety considerations of both boiling and pressurized systems. A break in a primary coolant pipe causes two-phase critical flow in either system since even in a pressurized water reactor, the reduction of pressure of the hot coolant from about 2,000 psia to near atmospheric causes flashing and two-phase flow. This kind of break results in a rapid loss of coolant and is considered to be the *maximum credible accident* in power reactors built to date.

The loss of coolant exposes the core to a steam environment. Even when the reactor is shutdown in time, the decay of fission products would, in the absence of adequate emergency cooling, release sufficient energy to heat the cladding to a temperature at which cladding metal-steam chemical reactions can take place. The combined decay and chemical reaction heating may result in core melting. An evaluation of the rate of flow in critical two-phase systems is therefore of importance for the design of emergency cooling and for the determination of the extent and causes of damage in accidents.

12-12. SINGLE-PHASE CRITICAL FLOW

Again it is instructive to begin the analysis with single-phase flow. Compressible, one-dimensional horizontal flow with no work or heat transfer will be assumed. The continuity and momentum equations are

$$\dot{m} = \rho AV \quad (12-68)$$

and

$$d(pA) + \frac{\dot{m}}{g_c} dV = dF \quad (12-69)$$

where F is a frictional force, A is the cross-sectional area and p is the pressure. Ignoring friction (isentropic flow) and combining the above two equations yields for constant A :

$$\frac{dV}{dp} + \frac{g_c}{\rho V} = 0 \quad (12-70)$$

The continuity equation is now differentiated with respect to p (with $dA/dp = 0$) to give

$$\frac{1}{\dot{m}} \frac{d\dot{m}}{dp} = \frac{1}{\rho} \frac{d\rho}{dp} + \frac{1}{V} \frac{dV}{dp} \quad (12-71)$$

When critical flow is reached the mass flow rate becomes a maximum, \dot{m}_{\max} , and $d\dot{m}/dp = 0$ in isentropic flow. Thus

$$\frac{1}{V} \frac{dV}{dp} = - \frac{1}{\rho} \frac{d\rho}{dp}$$

or

$$\frac{dV}{dp} = - \frac{\dot{m}_{\max}}{\rho^2 A} \frac{d\rho}{dp} \quad (12-72)$$

Combining Eqs. 12-68, 12-70, and 12-72 and rearranging give

$$\left(\frac{\dot{m}_{\max}}{A}\right)^2 = g_c \rho^2 \frac{dp}{d\rho} \quad (12-73a)$$

The above equation is written in the more usual form

$$G_{\max}^2 = -g_c \frac{dp}{dv} \quad (12-73b)$$

where G is the mass velocity m/A and v the specific volume ($v = \rho^{-1}$, $d\rho/dv = -\rho^2$). Equation 12-73b is identical to the equation for the speed of sound in isentropic flow, indicating that sonic velocity is reached in critical flow.

We shall now consider the energy equation (no heat transfer or work)

$$dh + \frac{VdV}{g_c J} = 0 \quad (12-74)$$

which integrates to

$$h_0 = h + \frac{V^2}{2g_c J} \quad (12-75)$$

where h and h_0 are the specific enthalpy and stagnation enthalpy of the fluid and J is Joule's equivalent, 778.16 ft lb_f/Btu. Thus

$$V = \sqrt{2g_c J (h_0 - h)} \quad (12-76)$$

The above equation applies whether the process is reversible or not. For an ideal gas $dh = c_p dT$, so that it becomes

$$\begin{aligned} V &= \sqrt{2g_c J c_p (T_0 - T)} \\ &= \sqrt{2g_c J c_p T_0 \left(1 - \frac{T}{T_0}\right)} \end{aligned} \quad (12-77)$$

where T_0 is the stagnation temperature. Recalling that for an ideal gas $T/T_0 = (p/p_0)^{(\gamma-1)/\gamma}$ (reversible) and $\rho = p/RT = (p_0/RT_0)(p/p_0)^{1/\gamma}$, where γ is the ratio of specific heats, and applying the continuity equation, Eq. 12-77 becomes

$$\dot{m} = \frac{Ap_0}{RT_0} \sqrt{2g_c J c_p T_0 \left[\left(\frac{p}{p_0}\right)^{2/\gamma} - \left(\frac{p}{p_0}\right)^{\frac{\gamma+1}{\gamma}} \right]} \quad (12-78)$$

where p_0 is the stagnation pressure and R the gas constant. This equation plots as *abd* in Fig. 12-19 if the pressure ratio p/p_0 were assumed to vary between 1.0 and 0. However, only the back-pressure ratio p_b/p_0 can vary between 1.0 and 0. The channel exit pressure p_e follows p_b as it is lowered until it reaches the critical value p_e^* indicated by the *critical pressure ratio* $r_p^* = p_e^*/p_0$, Fig. 12-19, and remains fixed for all values of

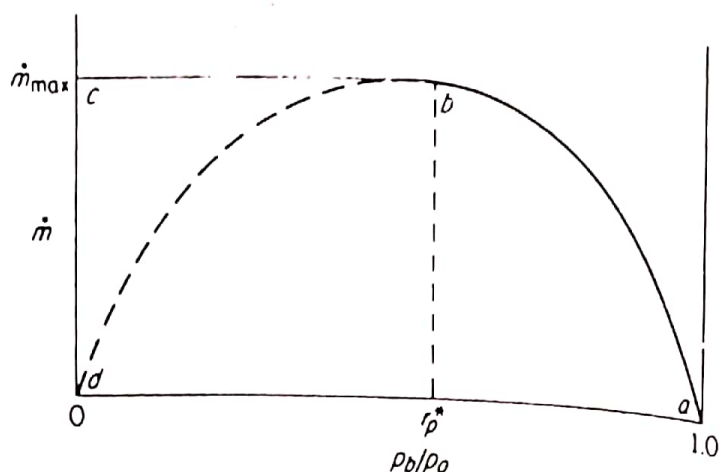


FIG. 12-19. Effect of pressure ratio on mass-flow rate.

p_b below this as indicated earlier. Also, the mass-flow rate increases as p_b/p_0 is lowered, reaches its maximum value \dot{m}_{\max} at r_p^* and remains fixed for all values of p_b/p_0 below r_p^* . The actual flow curve, therefore is abc in Fig. 12-19. The flow between b and c , again, is critical, restricted, or choked.

The value of r_p^* can be obtained by differentiating \dot{m} in Eq. 12-78 with respect to p and equating to zero. This results in

$$r_p^* = \left(\frac{2}{\gamma + 1} \right)^{\gamma/(\gamma - 1)} \quad (12-79)$$

A representative value of r_p^* is 0.53 for air at low temperatures ($\gamma = 1.4$). Thus if the upstream pressure is 100 psia, for example, a back pressure of 53 psia or lower would cause critical or choked flow. While steam is not a perfect gas, r_p^* for single-phase steam flow is approximated from the perfect gas relationship Eq. 12-79 by replacing γ with 1.3 for superheated and supersaturated or metastable (a case where actual condensation lags behind theoretical condensation in rapid expansion) steam, resulting in an r_p^* value of 0.545.

12-13. TWO-PHASE CRITICAL FLOW

For frictionless liquid and vapor flow, the momentum equations, for the same pressure drop, are

$$d(pA_f) + \frac{1}{g_c} d(\dot{m}_f V_f) = 0$$

or
$$d(pA_f) + \frac{1}{g_c} d(\rho_f A_f V_f^2) = 0 \quad (12-80)$$

and
$$d(pA_g) + \frac{1}{g_c} d(\rho_g A_g V_g^2) = 0 \quad (12-81)$$

where now the flow areas, densities and mass-flow rates of liquid and vapor are variable. The above equations are added to give

$$dp = -\frac{1}{g_c A} d[(\rho_f A_f V_f^2) + (\rho_g A_g V_g^2)] \quad (12-82)$$

where $A_f + A_g = A$, the channel total area. Using the continuity equations for the two phases, Eqs. 12-43, and the relationships $A_g/A = \alpha$ and $A_f/A = (1 - \alpha)$, Eq. 12-82 becomes

$$dp = -\frac{G^2}{g_c} d \left[\frac{(1-x)^2}{\rho_f(1-\alpha)} + \frac{x^2}{\rho_g \alpha} \right] \quad (12-83a)$$

where G is the total mass velocity \dot{m}_t/A , and x and α are the quality and void fraction respectively. Using the lumped model of Fig. 12-4b, it can be shown that the specific volume of the mixture is related to v_f and v_g by

$$v = v_f \frac{1-x}{1-\alpha} = \frac{1-x}{\rho_f(1-\alpha)} \quad (12-84a)$$

and

$$v = v_g \frac{x}{\alpha} = \frac{x}{\rho_g \alpha} \quad (12-84b)$$

so that the quantity between the brackets in Eq. 12-83a is simply equal to v . Equation 12-83a reduces to

$$G^2 = -g_c \frac{dp}{dv} \quad (12-83b)$$

which is identical in form to Eq. 12-73b for single-phase flow.

12-14. TWO-PHASE CRITICAL FLOW IN LONG CHANNELS

It is assumed, as in single-phase flow, that critical flow occurs when the pressure gradient at channel exit has reached a maximum value. In long channels, residence time is sufficiently long and thermodynamic equilibrium between the phases is attained. The liquid partially flashes into vapor as the pressure drops along the channel, and the specific volume of the mixture v attains a maximum value at the exit. Since v is a function of both x and α , it must be a function of the slip ratio S . Different values of S therefore result in different values of G . Maximum pressure gradient (and maximum G) are therefore obtained at a slip ratio when $\partial v / \partial S = 0$. This model, called the *slip equilibrium model*, is suggested by Fauske [133]. It assumes thermodynamic equilibrium between the two phases, and therefore applies to long channels.

The slip ratio, Eq. 12-8, is now combined with v , the quantity in the brackets in Eq. 12-83a, to eliminate α , giving

$$v = \frac{1}{S} [v_f(1-x)S + v_g x] [1 + x(S-1)] \quad (12-85)$$

thus

$$\frac{\partial v}{\partial S} = (x - x^2) \left(v_f - \frac{v_g}{S^2} \right) \quad (12-86)$$

Equating the above to zero, the value of S giving maximum flow, S^* , is

$$S^* = \sqrt{\frac{v_g}{v_f}} \quad (12-87)$$

G_{\max}^2 can now be obtained by combining Eqs. 12-83b and 12-85 as

$$G_{\max}^2 = \frac{-g_c}{-\frac{d}{dp} \left\{ \frac{1}{S} [v_f(1-x)S + v_g x] [1 + x(S-1)] \right\}}$$

giving finally [102]

$$G_{\max}^2 = -g_c S^* / \left\{ [(1-x + S^*x)x] \frac{dv_g}{dp} + [v_g(1 + 2S^*x - 2x) + v_f(2xS^* - 2S^* - 2xS^{*2} + S^{*2})] \frac{dx}{dp} \right\} \quad (12-88)$$

in which the term dv_f/dp has been neglected. The value of dv_g/dp can be approximated as $\Delta v_g/\Delta p$ for small Δp at p , or obtained from Fig. 12-20 for the water-steam system. The value of dx/dp at constant enthalpy is obtained from

$$h = h_f + xh_{fg}$$

Rearranging,

$$x = \frac{h - h_f}{h_{fg}} \quad (12-89)$$

Differentiating with respect to p ,

$$\begin{aligned} \frac{dx}{dp} &= d(h/h_{fg})/dp - d(h_f/h_{fg})/dp \\ &= \frac{1}{(h_{fg})^2} \left[\left(h_{fg} \frac{dh}{dp} - h \frac{dh_{fg}}{dp} \right) - \left(h_{fg} \frac{dh_f}{dp} - h_f \frac{dh_{fg}}{dp} \right) \right] \end{aligned}$$

The enthalpy of the water-steam mixture will not change with pressure, so that $dh/dp = 0$. Using $h_{fg} = h_g - h_f$, so that $dh_{fg} = dh_g - dh_f$, we can rewrite the above equation in the form

$$\frac{dx}{dp} = - \left(\frac{1-x}{h_{fg}} \frac{dh_f}{dp} \right) - \left(\frac{x}{h_{fg}} \frac{dh_g}{dp} \right) \quad (12-90)$$

As indicated above, the derivatives dh_f/dp and dh_g/dp are sole functions of the pressure. They are given in Fig. 12-20 for the ordinary-

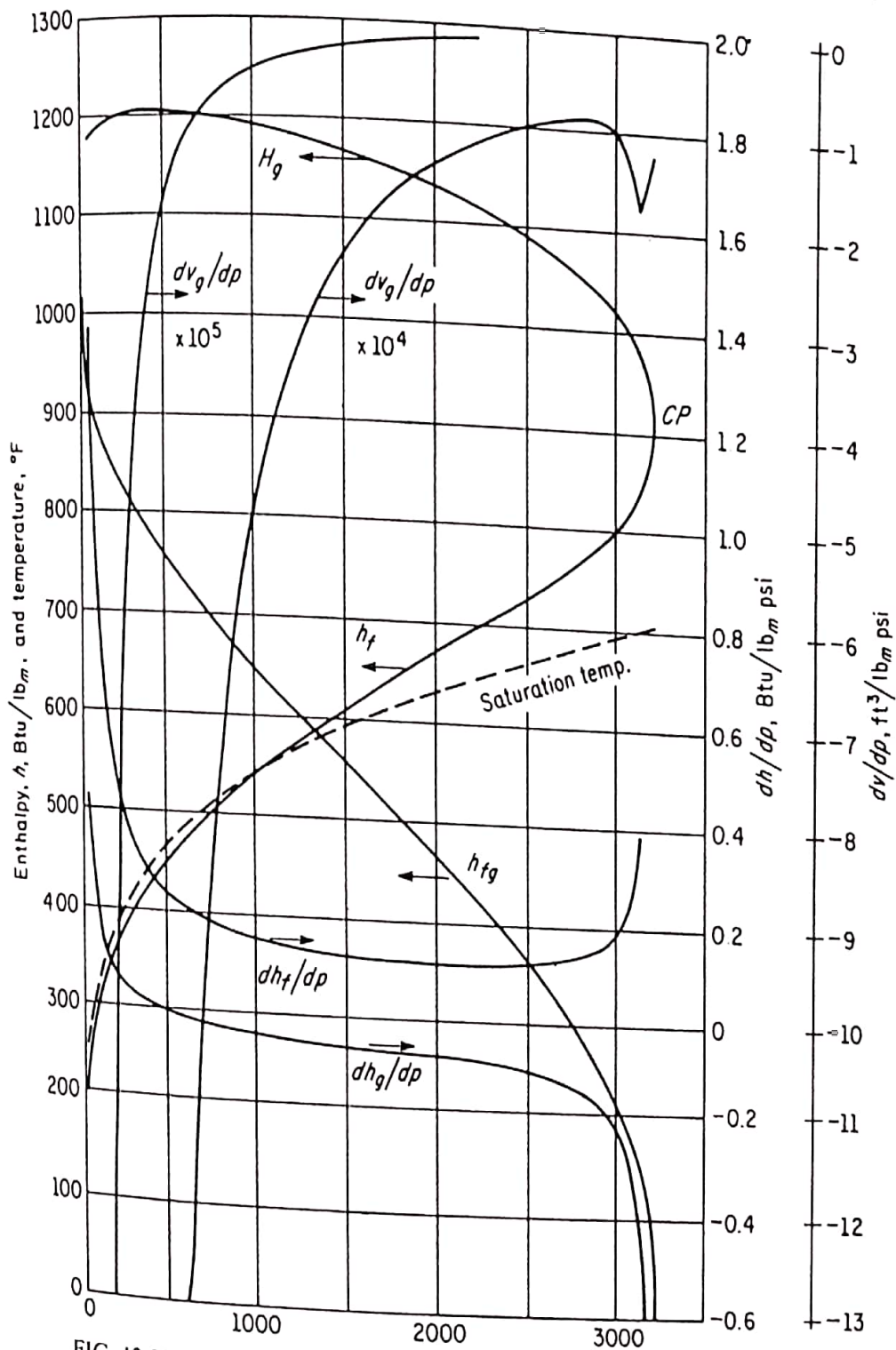


FIG. 12-20. Some thermodynamic properties of saturated water and steam.

water-steam system. The value of x is obtained from the energy equation 12-75 written for the two phases as follows

$$h_0 = (1 - x) \left(h_f + \frac{V_f^2}{2g_c J} \right) + x \left(h_g + \frac{V_g^2}{2g_c J} \right) \quad (12-91a)$$

This equation can be rewritten in terms of mass velocity G and slip ratio S as

$$h_0 = (1 - x)h_f + xh_g + \frac{G^2}{2g_c J} [(1 - x)Sv_f - xv_g]^2 \left[x + \frac{1 - x}{S^2} \right] \quad (12-91b)$$

where v_f , h_f , v_g and h_g are evaluated at the critical pressure. The latter can be determined from experimental data by Fauske [134]. This data was run on 0.25 in. ID channels with sharp-edged entrances having length-to-diameter, L/D , ratios between 0 (an orifice) and 40, and is believed to be independent of diameter alone. The critical pressure ratio was found to be approximately 0.55 for long channels in which the L/D ratio exceeds 12, region III in Fig. 12-21. This is the region in which the

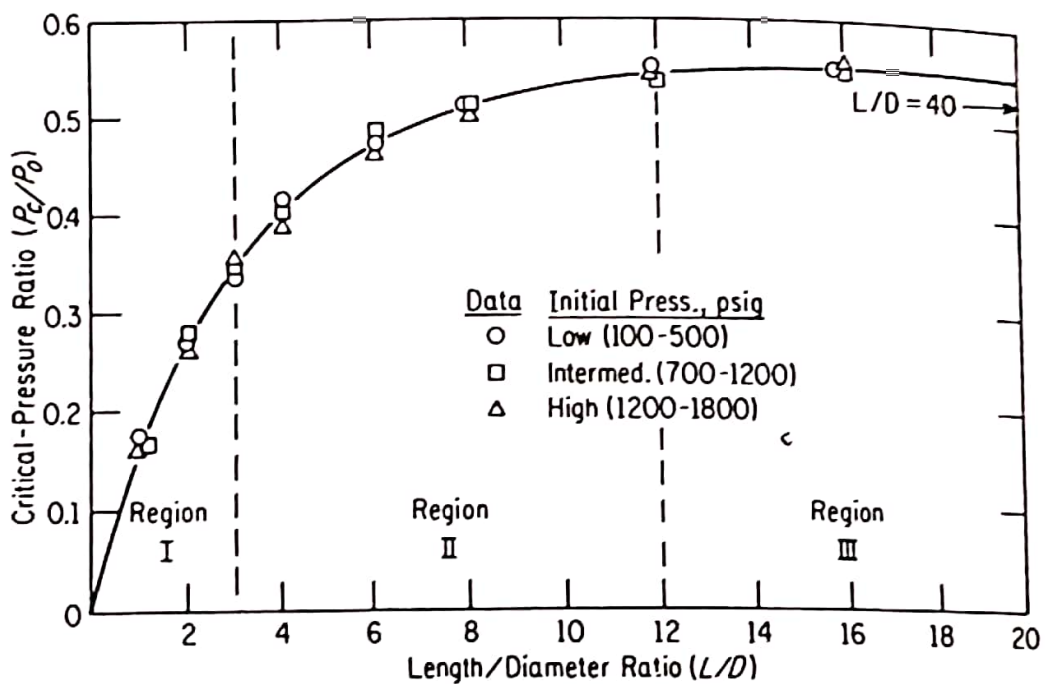


FIG. 12-21. Experimental critical pressure ratio data as a function of length/diameter ratio (Ref. 134).

Fauske slip-equilibrium model has been found applicable. The critical pressure ratio has been found to vary with L/D , for shorter channels, but appears to be independent of the initial pressure in all cases.

Solutions for the set of equations defining the Fauske slip-equilibrium model have been prepared by Fauske and are presented in Fig. 12-22.

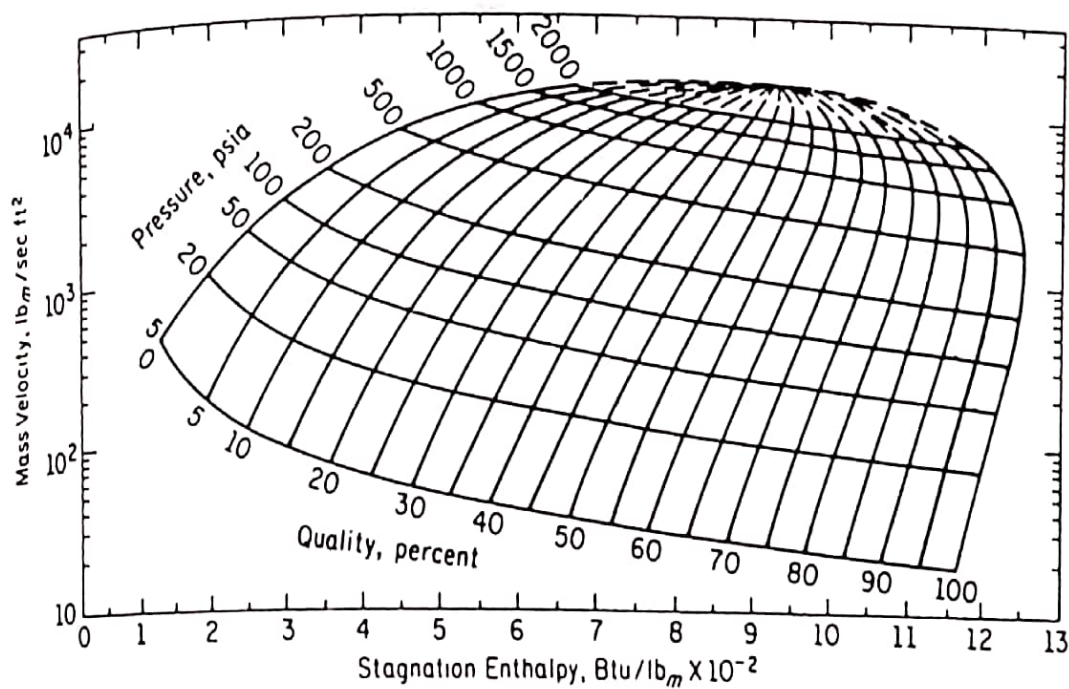


FIG. 12-22. Predictions of critical steam-water flow rates with slip equilibrium model (Ref. 134).

The critical flow is described by the local conditions at the channel exit. The flow is seen to increase with increasing pressure and with decreasing quality at the exit.

The Fauske model assumes thermodynamic equilibrium (no metastability, below), a case which due to the duration of flow, applies to long flow channels. Experimental data by many investigators showed the applicability of the Fauske model to L/D ratios above 12.

12-15. TWO-PHASE CRITICAL FLOW IN SHORT CHANNELS

Flashing of liquid into vapor, if thermal equilibrium is maintained, occurs as soon as the liquid moves into a region at a pressure lower than its saturation pressure. Flashing, however, could be delayed because of the lack of nuclei about which vapor bubbles may form, surface tension which retards their formation, due to heat-transfer problems, and other reasons. When this happens, a case of *metastability* is said to occur. Metastability occurs in rapid expansions, particularly in short flow channels, nozzles, and orifices.

The case of *short channels* has not been completely investigated analytically. The experimental data obtained in [134] covered both long and short tubes, $0 < L/D < 40$. For L/D between 0 and 12 the critical pressure ratios depend upon L/D , unlike long channels, Fig. 12-21.

For *orifices* ($L/D = 0$) the experimental data showed that because residence time is short, flashing occurred outside the orifice (Fig. 12-23a)

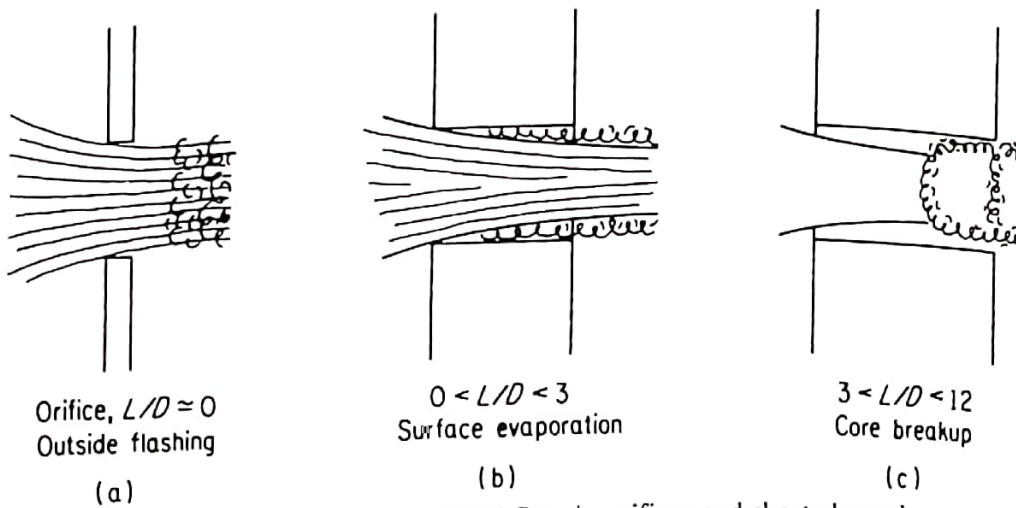


FIG. 12-23. Two-phase critical flow in orifices and short channels.

and no critical pressure existed. The flow is accurately determined from the incompressible flow orifice equation

$$G = 0.61 \sqrt{2g_c \rho (p_0 - p_b)} \quad (12-92)$$

For region I, Fig. 12-21, $0 < L/D < 3$, the liquid immediately speeds up and becomes a metastable liquid core jet where evaporation occurs from its surface, Fig. 12-23b. The flow is determined from

$$G = 0.61 \sqrt{2g_c \rho (p_0 - p_c)} \quad (12-93)$$

where p_c is obtained from Fig. 12-21.

In region II, $3 < L/D < 12$, the metastable liquid core breaks up, Fig. 12-23c, resulting in high-pressure fluctuations. The flow is less than would be predicted by Eq. 12-93. Figure 12-24 shows experimental critical flows for region II.

All the above data were obtained on sharp entrance channels. In rounded-entrance channels the metastable liquid remains more in contact with the walls and flow restriction requires less vapor. For $0 < L/D < 3$ channels, such as *nozzles*, the rounded entrances result in much higher critical pressure ratios than indicated by Fig. 12-21 as well as somewhat greater flows [135]. The effect of rounded entrances is negligible for long channels ($L/D > 12$) so that the slip-equilibrium model can be used there. The effect of L/D ratio on flow diminishes between 3 and 12.

The condition of the wall surface is not believed to affect critical flow in sharp-entrance channels, since the liquid core is not in touch with the walls and evaporation occurs at the core surface or by core breakup. It will have some effect on rounded-entrance channels. The existence of gases or vapor bubbles will affect the flow also, since they will act as nucleation centers [136].

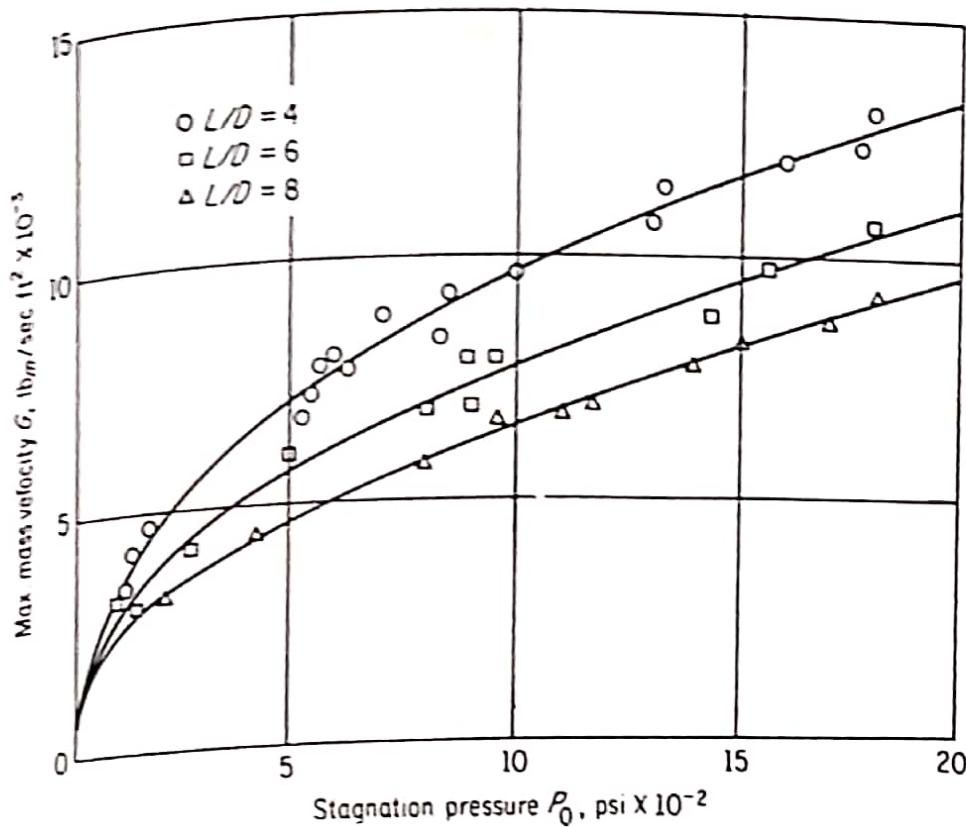


FIG. 12-24. Experimental two-phase critical flow rates for region II of Fig. 12-21.

PROBLEMS

12-1. Water enters a 6-ft-long uniformly heated 1-in. tube at 460°F and 600 psia. The entrance velocity is 2.5 fps. Neglecting pressure losses in the channel, determine the maximum heat input, in Btu/hr ft of channel length, if the exit void fraction is not to exceed 60 percent.

12-2. A boiling-water reactor operates at 600 psig. In one of its channels the inlet velocity is 1.4 fps, the heat generated is 5×10^6 Btu/hr, and the total coolant flow is 76,000 lb_m/hr . The incoming water is 11°F subcooled. Estimate the exit void fraction in that channel.

12-3. A boiling-sodium, graphite-moderated reactor core operates at an average pressure of 15.4 psia. The average slip ratio is 4. Sodium enters the core at 1140°F and leaves with an average void fraction of 80 percent. Determine the amount of heat added per pound mass of coolant.

12-4. A boiling-sodium reactor channel, 1 in.² cross-sectional area, operates at an average pressure of 9.153 psia. Subcooled sodium enters the channel at 1900 °R and 20 fps. 2.37×10^6 Btu/hr are added in the channel. The exit void fraction is 96 percent. What is the slip ratio?

12-5. A 12-ft-high boiling-water reactor channel operating at 1,200 psia with sinusoidal heat generation has a nonboiling height of 4 ft. The inlet water is 27.22°F subcooled. Find the exit quality of the channel.

12-6. A 6-ft-high boiling-water reactor channel operates at an average pressure of 700 psia. Water enters the channel 23.1°F subcooled and leaves

with a 6 percent steam quality. Calculate the nonboiling and boiling heights if heat is added along the channel (a) uniformly and (b) sinusoidally. Neglect the extrapolation lengths.

12-7. A 6-ft-high boiling-water channel operates at 700 psia average, 23.1°F subcooling, and 6 percent exit quality (as above). The voids in the upper part of the channel, however, cause strong neutron-flux depression there, so that the axial flux distribution is represented by

$$\varphi = Ce^{-\pi z/H} \sin \frac{\pi z}{H}$$

where C is a constant, $z = 0$ indicates the channel entrance, and H is the channel height. Find (a) the height z at which the flux is maximum, (b) the value of C in terms of the maximum flux, and (c) the nonboiling and boiling heights.

12-8. A 5-ft-high boiling-water channel is 4.25 in. by 0.45 in. in cross section. Heat is added sinusoidally at an average pressure of 600 psia. Water enters the channel 5 Btu/lb_m subcooled at 2 fps and leaves with a void fraction of 32.9 percent. Neglecting the extrapolation lengths, calculate the power density in kilowatts per liter of coolant volume (a) in the entire channel and (b) in the boiling height only.

12-9. A boiling-water reactor channel operates at 1,000 psia, with 19.6°F subcooling and 10 percent exit quality. The acceleration pressure drop is 0.1 psi. The slip ratio is 2. Compute the amount of heat added in the channel in Btu/hr if the channel cross-sectional area is 3 in.².

12-10. A 4-ft-high boiling-water channel is 4.5 in. by 0.5 in. in cross section. It receives heat uniformly at the rate of 3×10^5 Btu/hr ft² of wide sides only. The average channel pressure is 1,200 psia. Water enters the channel saturated at 2 fps. For a slip ratio of 2 and a friction factor of 0.03, calculate the friction and acceleration pressure drops in the channel.

12-11. A 5-ft-high boiling-water channel has an equivalent diameter of 0.5 in. Water enters the channel at the rate of 2×10^5 lb_m/hr at 10 fps (forced circulation), 22°F subcooled. Five Mw(t) of heat are added sinusoidally in the channel. The slip ratio is 1.8, and the average pressure is 900 psia. Neglecting the extrapolation lengths, calculate the friction and acceleration pressure drops. Consider the cladding surface to correspond to smooth-drawn tubing.

12-12. A 12-ft-high BWR channel operates at 800 psia and 18.23°F subcooling. The nonboiling height is 4 ft. The slip ratio is 2. The exit quality is 20 percent. The friction factor is 0.015. The equivalent diameter in the channel is 0.14 ft. (a) Find the acceleration pressure drop if the friction pressure drop is 10 lb_f/ft². (b) Find the power generated in the channel in Mw(t) per ft² of channel-flow area.

12-13. A boiling-water channel has a cross-sectional area of 0.025 ft². It operates at 1,000 psia, receives saturated inlet water and has an exit quality of 10 percent. The slip ratio is 3. The acceleration pressure drop is 0.1 psi. How much heat is generated in the channel in Btu/hr?

12-14. A 10-ft-high channel in a 1,000-psia boiling-water reactor generates 2×10^5 Btu/hr uniformly. It has an equivalent diameter of 0.15 ft. The inlet

water has a velocity of 6 fps and is 24.61°F subcooled. The water mass-flow rate is $2000 \text{ lb}_m/\text{hr}$ and the slip ratio is 3.0. Find the friction pressure drop in that channel if the friction factor is 0.015.

12-15. A vertical fuel element in a boiling-water reactor is in the form of a thin cylindrical shell 2 in. ID. Water flowing upward enters at core bottom 22°F subcooled. The inlet water speed on the inside of the cylinder is 3 fps. The average pressure within the element is 900 psia. The portion of the heat generated by the element and conducted radially inward is 10^6 Btu/hr . The slip ratio is 2.0. The element support at the top is such that there is a sudden reduction in the inside diameter to 1.7 in., followed by a sudden expansion back to 2.0 in. Calculate the net pressure change due to this obstruction. The obstruction may be considered long enough so that the pressure changes are additive.

12-16. A 2-in.-diameter, two-phase flow channel has an obstruction in it in the form of a concentric 1-in.-diam. disk. The pressure drop due to the obstruction is 0.1 psf at a total mass-flow rate of $124.3 \text{ lb}_m/\text{hr}$, and a pressure of 600 psia. What is the quality at the obstruction? Take $C_D = 0.6$. The fluid is water.

12-17. $100 \text{ lb}_m/\text{hr}$ of saturated water enter a 1-in.-diam. boiling channel at 1,000 psia. At a point where $3,247 \text{ Btu/hr}$ have been added in the channel, a restriction in the form of a 0.2-in.-diam. orifice exists. Calculate the pressure drop due to the restriction if $C_D = 0.6$.

12-18. A PWR pressure vessel is connected to a heat exchanger via a long pipe. The pressure in the vessel is 2,000 psia. A break occurred at the end of the pipe. At the break, the quality was found to be 5 percent. What is the void fraction at the same location?

12-19. A small hole, 0.02 ft^2 in area, developed in the core shroud of a natural-circulation BWR. Two-phase mixture at 800 psia and 10 percent quality spilled into the downcomer. The downcomer is at 799 psia. The coefficient of discharge through the hole can be taken as 0.6. What is the rate of spillage in lb_m/hr ?

12-20. A 12-in.-diam. primary coolant pipe carries 2,000 psia, 560°F water from the pressure vessel of a PWR. A sudden clean break is presumed to have occurred 2 ft. from the vessel. Calculate the initial rate of coolant loss in lb_m/sec .

12-21. A PWR operates at 2,000 psia and 580°F average water temperature. The outlet pipe is 1 ft in diam. A sudden break occurred about 20 ft from the vessel. The break is clean and perpendicular to the pipe axis. The back pressure is atmospheric. Calculate the rate of coolant loss in lb_m/sec at the instant the break occurred.